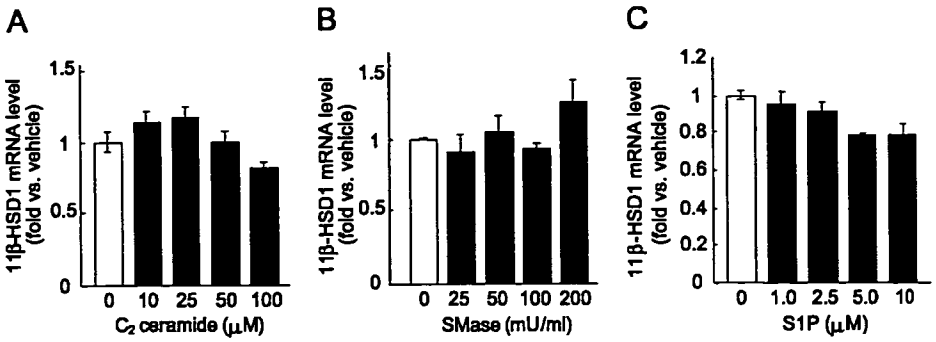

FIG. 3. Ceramide does not influence the expression of 11β-HSD1 in differentiated 3T3-L1 adipocytes. mRNA level of 11β-HSD1 after treatment with C_2 ceramide (10–100 μM) (A), SMase (25–200 mU/ml) (B), and S1P (1.0–10 μM) (C) for 24 h. Results are means ± SEM from three independent experiments.

been investigated exclusively in hepatocytes (40). Because C/EBPα is not expressed in preadipocytes (41), we tested a possibility that C/EBPβ would be involved in the regulation of 11β-HSD1 by ceramide or AICAR. Western blot analysis showed that C/EBPβ expression was substantially increased after the treatment with C_2 ceramide (0.1 mM) or AICAR (0.5 mM), culminating in 1.8- and 6.5-fold increase within 3 h, respectively (Fig. 7, A and B). Expression of C/EBPβ by C_2 ceramide or AICAR was increased in a dose-dependent manner (data not shown). In contrast, 11β-HSD1 expression was induced 12 h after the treatment with C_2 ceramide or AICAR (data not shown).

To explore a possible involvement of C/EBPβ in 11β-HSD1 regulation, ChIP analysis was performed with primers spanning putative C/EBP binding sites in mouse 11β-HSD1 promoter (30). No amplified band was observed in samples processed without antibody (No antibody control), excluding a possibility of nonspecific binding between DNA fragments and protein A-agarose (Fig. 7C). When treated with C_2 ceramide or AICAR for 6 h, association of C/EBPβ with the promoter of 11β-HSD1 gene was substantially induced (Fig. 7C). Our data demonstrated that the activation of ceramide or AMPK pathways induced the expression of C/EBPβ and its binding to the 11β-HSD1 promoter.

Effect of C/EBPβ knockdown on the expression of 11β-HSD1 induced by ceramide or AMPK signaling in 3T3-L1 preadipocytes

To further validate a role of C/EBPβ in the control of 11β-HSD1 by ceramide or AICAR, C/EBPβ protein was transiently knocked down by siRNA. When 3T3-L1 preadipocytes were transfected with siRNA, C/EBPβ protein expression induced by C_2 ceramide or AICAR was markedly attenuated, demonstrating effective silencing of C/EBPβ (Fig. 8, A and B). Notably, augmented expression of 11β-HSD1 induced by C_2 ceramide or AICAR was significantly attenuated in cells transfected with C/EBPβ siRNA (Fig. 8,

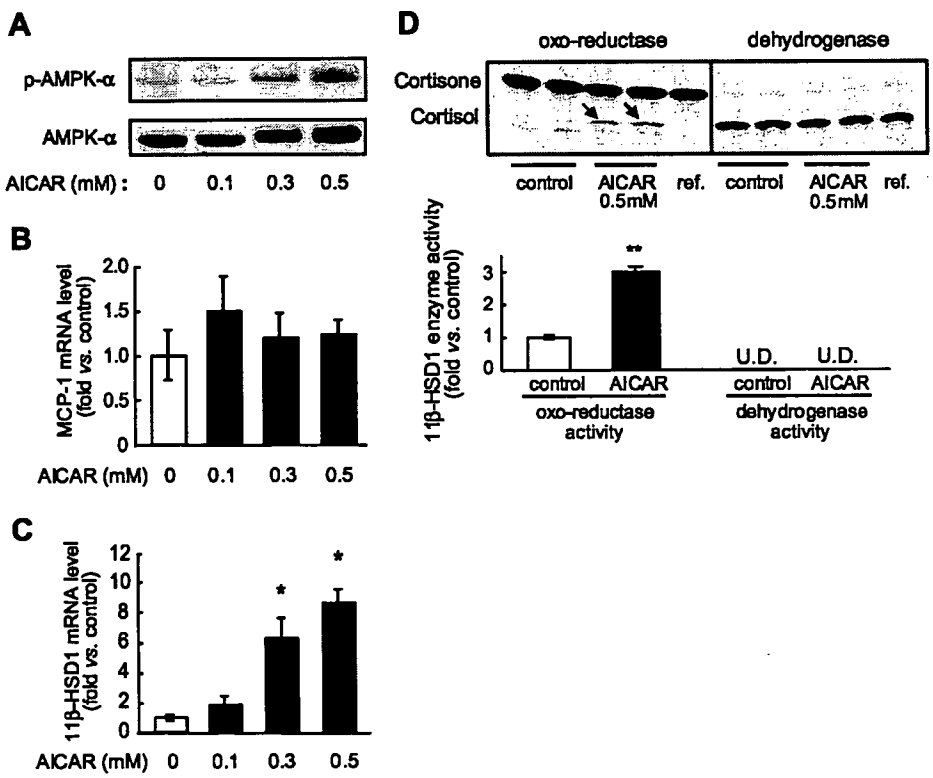

FIG. 4. AMPK activation enhances the expression of 11β-HSD1 in 3T3-L1 preadipocytes. Cells were treated with AICAR (0.1–0.5 mM) for 24 h. A, Western blot of AMPK protein and phosphorylated AMPK (p-AMPK). mRNA levels of MCP-1 (B) and 11β-HSD1 (C). D, Assay for 11β-HSD1 activity. Cells treated with AICAR (0.5 mM) for 24 h were incubated in serum-free media containing 250 nM of cortisone or cortisol with tritium-labeled tracer (6.4 μCi/ml of [1,2-^{3}H]$_2$ cortisone or [1,2,6,7-^{3}H]$_4$ cortisol) for 12 h. Emerged spots of cortisol were indicated by *arrows*. Results are means ± SEM from three or four experiments. *, $P < 0.05$, **, $P < 0.01$ compared with control (cells without AICAR treatment) group. U.D., Under detectable.

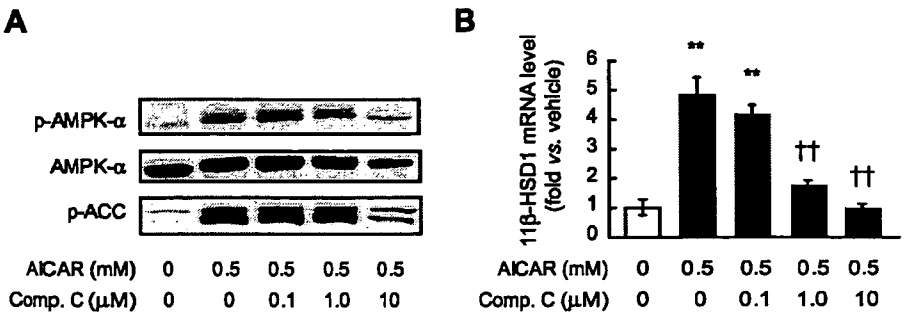

FIG. 5. AICAR-induced expression of 11β-HSD1 is attenuated by an AMPK inhibitor. 3T3-L1 preadipocytes were cotreated with AICAR (0.5 mM) and indicated concentrations of compound C (Comp. C) for 24 h. A, Western blot of total AMPK protein, phosphorylated AMPK (p-AMPK) and phosphorylated ACC (p-ACC). B, mRNA level of 11β-HSD1. Results are means ± SEM from three experiments. **, $P < 0.01$ compared with vehicle-treated group. ††, $P < 0.01$ compared with AICAR-treated group.

C and D). In contrast, negative control Stealth RNAi treatment had no impact on the expression of C/EBPβ or 11β-HSD1. These results suggest that C/EBPβ is involved critically in the induction of 11β-HSD1 by ceramide- or AMPK-mediated signaling pathways.

Discussion

The major finding of the present study is that ceramide- and AMPK-mediated signaling pathways augment the expression and enzyme activity of 11β-HSD1 in both murine and human preadipocytes. We provide novel evidence that activation of ceramide and AMPK pathways induce the expression of C/EBPβ. ChIP analyses demonstrate the DNA binding of C/EBPβ to 11β-HSD1 promoter, and transient knockdown of C/EBPβ protein by siRNA further support the notion that C/EBPβ is critically involved in the expression of 11β-HSD1 induced by C_2 ceramide or AICAR. Taken together, the present study highlights a novel mechanism that metabolic stress-related signaling pathways mediated by ceramide and AMPK regulate the expression of 11β-HSD1 in preadipocytes.

Ceramide acts as a lipid mediator of metabolic stress response (18, 42). Fatty acids, proinflammatory cytokines, glucocorticoids, and serum deprivation in cultured cells are known to induce intracellular accumulation of ceramide (43, 44). Importantly, aberrant accumulation of ceramide in insulin target tissues appreciably contributes to local insulin resistance and underlies, at least partly, the molecular mechanism of lipotoxicity (43, 44). A recent study demonstrated that mRNA level of enzymes involved in sphingolipid metabolism in adipose tissue as well as plasma level of SMase, ceramide, sphingosine, and S1P were increased in *ob/ob* mice (45). Thus we tested a possibility whether 11β-HSD1 would be induced by ceramide signals in preadipocytes. In this context, the present study is the first to demonstrate that the expression of 11β-HSD1 was induced by C_2 ceramide, bacterial SMase and S1P in preadipocytes (Fig. 2). In contrast, induction of 11β-HSD1 expression by C_2 ceramide, SMase, and S1P was not observed in differentiated adipocytes (Fig. 3), suggesting that such effects are restricted in preadipocytes.

SMase catalyzes the hydrolysis of sphingomyelin in outer side of the plasma membrane, leading to the production of ceramide (19). Ceramide is subsequently metabolized to S1P, which functions through S1P receptors (19). In the present study, we found that inhibition of SMase by desipramine attenuated the TNFα- or IL-1β-induced expression of 11β-HSD1. This observation is in agreement with previous reports that TNFα and IL-1β promptly induced the hydrolysis of sphingomyelin to generate ceramide (46). Assays in the present study are validated by the finding that expression of MCP-1 was induced by C_2 ceramide (Fig. 2), consistent with the notion that NFκB and MAPK signaling pathways are involved in the regulation of MCP-1 (47) and that ceramide and S1P potently mediate NFκB and MAPK pathways (18, 48).

In the present study, C_2 ceramide induced the expression of 11β-HSD1 at 50–100 μM (Fig. 2). It has been reported that the physiological concentration of ceramide within cells are approximately 1–5 μM (49). Accordingly, C_2 ceramide does induce biological effects including differentiation and growth inhibition at 1–5 μM in serum-free media. However, higher concentration (50–100 μM) of C_2 ceramide are required to induce equipotent effects in serum-containing medium, because serum proteins bind C_2 ceramide and reduce its potency (50), and for this, 50–100 μM C_2 ceramide has been commonly used in many previous studies (51, 52). It should also be noted that, because ceramide resides in "lipid rafts" in the membrane (53), local concentration of ceramide within cells must be much higher than 5 μM. In this context, the concentration of C_2 ceramide used in the present study is appropriate for analyzing the responsiveness of ceramide in adipocytes.

AMPK, activated by the increase in intracellular AMP level, plays a crucial role in mediating cellular stress such as hypoxia, glucose deprivation, and ischemia (20–22). Recent studies highlighted a potential role of AMPK in regulating energy balance and mass of adipose tissue (23, 24). ATP level of adipose tissue is decreased in obese rodent models (54), supporting the notion that local hypoxia and inflammation is associated with defective energy metabolism in obese adipose tissue (14, 54). In this context, the present study demonstrates for the first time that AICAR markedly augmented the expression of 11β-HSD1 in preadipocytes (Fig. 4). Furthermore, a potent AMPK inhibitor compound C completely suppressed the induction of 11β-HSD1 (Fig. 5), verifying that AMPK signaling pathway is involved in the regulation of 11β-HSD1. Based on the present study in 3T3-L1 preadipocytes (Figs. 2, 4, and 5), a potential interaction between ceramide and AMPK in terms of the effect on 11β-HSD1 expression would be of considerable interest. In 3T3-L1 preadipocytes, AMPK was not activated when treated with C_2 ceramide (data not shown). Although further studies are required, these results suggest that ceramide signal is not directly involved in AMPK-mediated induction of 11β-HSD1.

The present study is the first to demonstrate that C_2 cer-

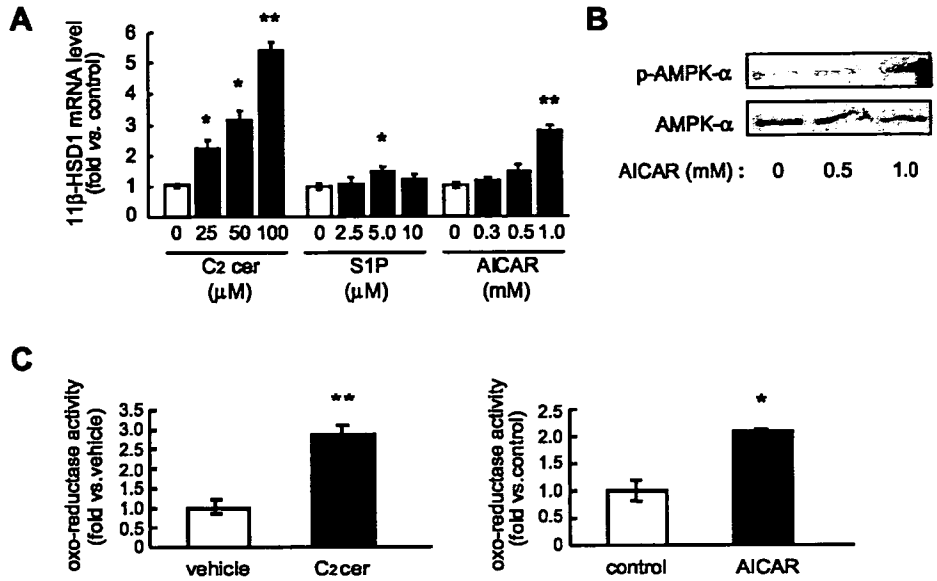

FIG. 6. Ceramide and AMPK signaling induces the expression of 11β-HSD1 in human preadipocytes. Human preadipocytes were treated with C_2 ceramide (C_2cer, 25–100 μM), S1P (2.5–10 μM) and AICAR (0.3–1.0 mM) for 24 h. A, mRNA levels of 11β-HSD1 were determined. B, Western blot of AMPK protein and phosphorylated AMPK (p-AMPK) after treatment with AICAR for 3 h. C, Assay for 11β-HSD1 oxo-reductase activity. Cells were treated with C_2 ceramide (50 μM, *left*) or AICAR (1.0 mM, *right*) for 24 h, and subsequently incubated with tritium-labeled cortisone for 12 h. Results are means ± SEM from three experiments. *, $P < 0.05$, **, $P < 0.01$ compared with control or vehicle-treated group.

amide and AICAR augmented the expression of C/EBPβ in 3T3-L1 preadipocytes (Fig. 7). This result is consistent with a line of previous reports showing that S1P induced phosphorylation of cAMP-responsive-element-binding protein (CREB) (48), and CREB potentially controls the expression of C/EBPβ in adipocytes (55). Furthermore, the present study is the first demonstration that the activation of AMPK induced the expression of C/EBPβ in any kinds of cells. It is well-characterized that transient expression of C/EBPβ is essential for the induction of PPARγ and C/EBPα in the early phase of adipogenesis (41). A recent report raised a possibility that AICAR inhibited adipogenesis by interfering induction of PPARγ and C/EBPα (56). Therefore, it is tempting to speculate that AMPK-induced augmentation and sustainment of C/EBPβ and resultant suppression of adipogenesis may be a facet of adaptation to nutritional threat.

Compared with murine adipocytes, the mechanism responsible for adipogenesis and adipokine secretion is poorly understood in humans (57). For example, human preadipocytes do not require the process of clonal expansion in the course of adipogenesis (57). Therefore, we examined the effect of ceramide and AMPK signaling on the expression of 11β-HSD1 using human preadipocytes. The present study demonstrates that sphingolipids (C_2 ceramide and S1P) and AICAR induced the expression of 11β-HSD1 also in human preadipocytes (Fig. 6). The effect of C_2 ceramide was exaggerated in human preadipocytes compared with 3T3-L1 preadipocytes, whereas the effect of S1P was mild in human preadipocytes. Treatment of C_2 ceramide did not affect MCP-1 mRNA level, but AICAR substantially reduced the expression in a dose-dependent manner (data not shown), representing a contrast to the data in 3T3-L1 preadipocytes (Figs. 2 and 4). Even considering differences in cell types or species (58), our data provide novel evidence that ceramide and AMPK signals induce the expression of 11β-HSD1 in both rodent and human cultured preadipocytes. Recent

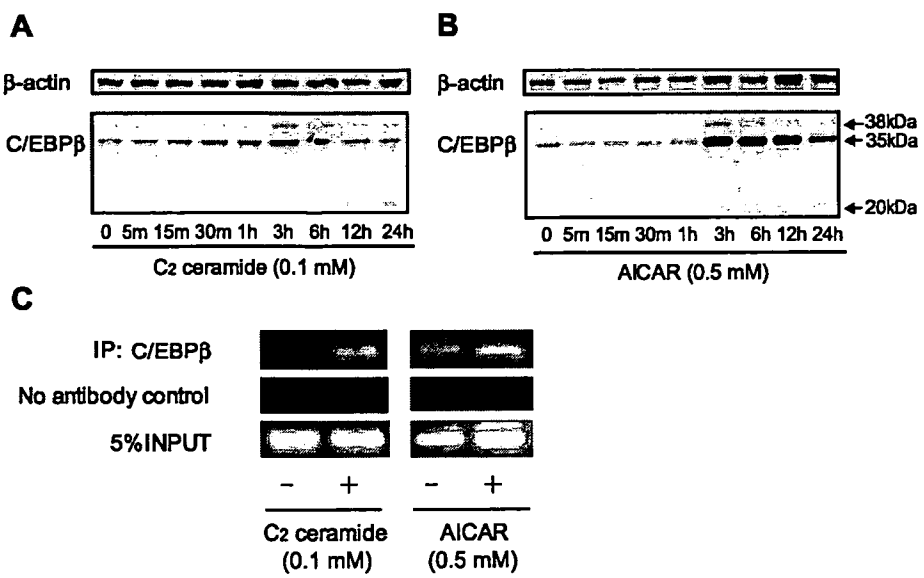

FIG. 7. Ceramide and AICAR induce the expression of C/EBPβ in 3T3-L1 preadipocytes. Western blot of C/EBPβ after the treatment with 0.1 mM C_2 ceramide (A) or 0.5 mM AICAR (B). β-Actin was used as a loading control. ChIP analysis after the treatment with 0.1 mM C_2 ceramide or 0.5 mM AICAR for 6 h (C). Chromatin-associated DNA was immunoprecipitated with an antibody against C/EBPβ. The immunoprecipitated DNA, samples processed without antibody (indicated as No antibody control), and 5% amount of sonicated DNA (indicated as 5% INPUT) were subjected to PCR using specific primers for 11β-HSD1 promoter region. Amplified DNA indicates the binding of C/EBPβ to the 11β-HSD1 promoter.

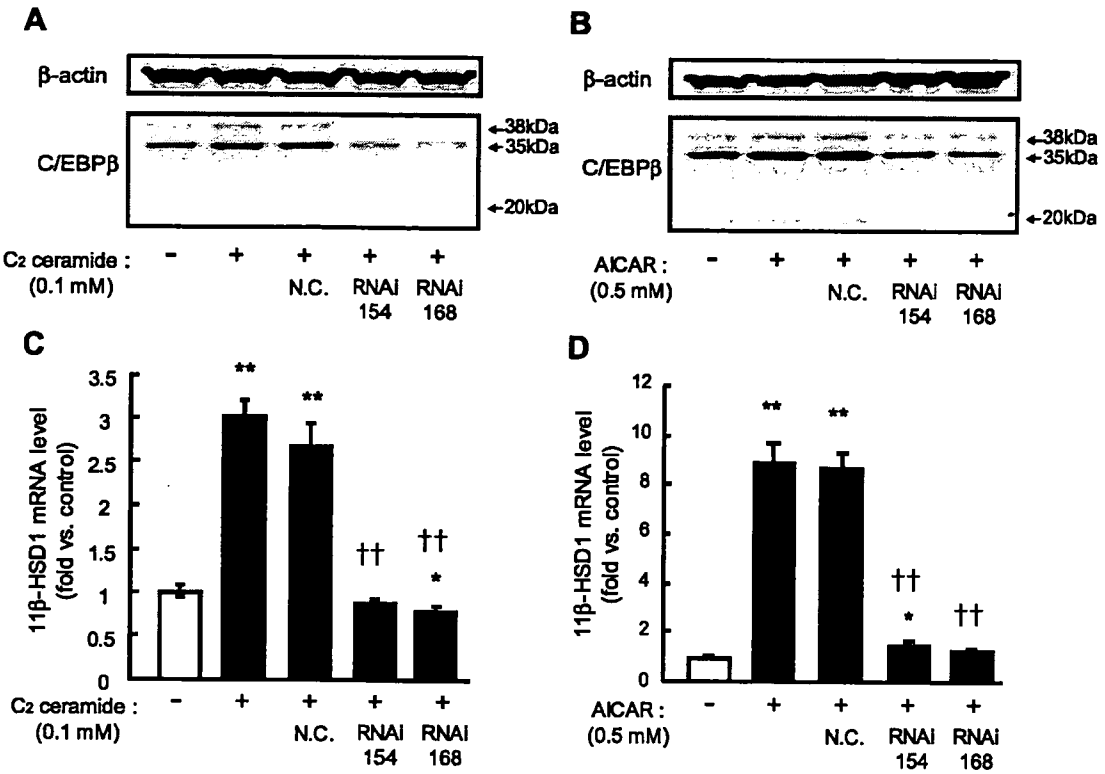

FIG. 8. Effect of C/EBPβ knockdown on C_2 ceramide- or AICAR-induced expression of 11β-HSD1 in 3T3-L1 preadipocytes. Cells were transfected with either Stealth RNAi negative control (N.C.) or C/EBPβ Stealth RNAi (RNAi154, RNAi168). After 12 h of incubation, cells were treated with C_2 ceramide or AICAR. Western blot of C/EBPβ after the treatment with 0.1 mM C_2 ceramide (A) or 0.5 mM AICAR (B) for 3 h. β-Actin was used as a loading control. mRNA level of 11β-HSD1 after the treatment with 0.1 mM C_2 ceramide (C) or 0.5 mM AICAR (D) for 24 h. Results are means ± SEM from four experiments. *, $P < 0.05$, **, $P < 0.01$ compared with control group. ††, $P < 0.01$ compared with C_2 ceramide or AICAR-treated group.

works demonstrated that human adipose tissue contained a considerable amount of preadipocytes (59, 60), which may be involved in some aspects of adipose tissue function (15, 60). In this context, further *in vivo* studies are warranted to validate the possible involvement of ceramide and AMPK signals in 11β-HSD1 regulation in human preadipocytes.

C/EBP family of transcription factors (C/EBPs) in adipocytes serve as master regulators of a variety of cellular response (61), and expression of C/EBPs is regulated by a variety of hormones, cytokines, and nutrients (61, 62). 11β-HSD1 promoter contains a couple of C/EBP binding sites, and previous studies demonstrated that the expression of 11β-HSD1 was controlled by C/EBPs (40, 63). In this context, the present study demonstrates, for the first time, that induction of C/EBPβ in preadipocytes was observed around 3 h after the treatment with C_2 ceramide or AICAR (Fig. 7), which preceded the robust induction of 11β-HSD1. Our data of ChIP analyses and C/EBPβ knockdown experiments further reinforced the notion that C/EBPβ is involved in ceramide- and AMPK-mediated augmentation of 11β-HSD1 in preadipocytes (Figs. 7 and 8).

It should be noted that glucocorticoid is known to increase the expression and activity of SMase, resulting in intracellular ceramide accumulation and local insulin resistance (43). This notion prompts us to speculate a vicious cycle within cells where ceramide and 11β-HSD1-derived active glucocorticoid reciprocally aggravate preadipocyte dysfunction. Unexpected regulation of 11β-HSD1 by AMPK pathway may also provide a novel clue to better understand molecular pathophysiology of adipose dysfunction. Collectively, the present study is the first demonstration that ceramide and AMPK signaling pathways augment the expression and enzyme activity of 11β-HSD1 in human and rodent preadipocytes, thereby highlighting a metabolic stress-related regulation of 11β-HSD1 in a cell-specific manner.

Acknowledgments

We thank Ms. S. Maki, K. Koyama, and M. Nagamoto for experimental assistance. We are grateful to Dr. S. Yokota and Mr. Y. Tominaga (Kaneka Corporation) for technical advice.

Received March 14, 2007. Accepted August 8, 2007.

Address all correspondence and requests for reprints to: Hiroaki Masuzaki, M.D., Ph.D., Division of Endocrinology and Metabolism, Department of Medicine and Clinical Science, Kyoto University Graduate School of Medicine, 54, Shogoin Kawahara-cho, Sakyo-ku, Kyoto 606-8507, Japan. E-mail: hiroaki@kuhp.kyoto-u.ac.jp.

This work was supported by Grant-in-Aid for Scientific Research (B2) (16390267); Grant-in-Aid for Scientific Research (S2) (16109007); Grant-in-Aid for Scientific Research on Priority Areas (Adipomics, 15081101); Grant-in-Aid for Research on Measures for Intractable Diseases (Health and Labor Science Research Grant); The Ministry of Education, Culture, Sports, Science and Technology of Japan; Research Grant from Special Coordination Funds for Promoting Science and Technology (Japan Science and Technology Agency); AstraZeneca International Research Grant; Takeda Medical Research Foundation; Smoking Research Foundation; Setsuro Fujii Memorial Osaka Foundation for Promotion of Fun-

damental Medical Research; Research Grant for Cardiovascular Diseases (National Cardiovascular Center); Mitsubishi Pharma Research Foundation; and Sankyo Research Foundation for Medical Research.

Disclosure Statement: The authors of this manuscript have nothing to disclose.

References

1. Grundy SM, Brewer Jr HB, Cleeman JI, Smith Jr SC, Lenfant C 2004 Definition of metabolic syndrome: report of the National Heart, Lung, and Blood Institute/American Heart Association conference on scientific issues related to definition. Circulation 109:433–438
2. Matsuzawa Y 2006 Therapy insight: adipocytokines in metabolic syndrome and related cardiovascular disease. Nat Clin Pract Cardiovasc Med 3:35–42
3. Masuzaki H, Paterson J, Shinyama H, Morton NM, Mullins JJ, Seckl JR, Flier JS 2001 A transgenic model of visceral obesity and the metabolic syndrome. Science 294:2166–2170
4. Masuzaki H, Yamamoto H, Kenyon CJ, Elmquist JK, Morton NM, Paterson JM, Shinyama H, Sharp MG, Fleming S, Mullins JJ, Seckl JR, Flier JS 2003 Transgenic amplification of glucocorticoid action in adipose tissue causes high blood pressure in mice. J Clin Invest 112:83–90
5. Kotelevtsev Y, Holmes MC, Burchell A, Houston PM, Schmoll D, Jamieson P, Best R, Brown R, Edwards CR, Seckl JR, Mullins JJ 1997 11β-Hydroxysteroid dehydrogenase type 1 knockout mice show attenuated glucocorticoid-inducible responses and resist hyperglycemia on obesity or stress. Proc Natl Acad Sci USA 94:14924–14929
6. Morton NM, Holmes MC, Fievet C, Staels B, Tailleux A, Mullins JJ, Seckl JR 2001 Improved lipid and lipoprotein profile, hepatic insulin sensitivity, and glucose tolerance in 11β-hydroxysteroid dehydrogenase type 1 null mice. J Biol Chem 276:41293–41300
7. Morton NM, Paterson JM, Masuzaki H, Holmes MC, Staels B, Fievet C, Walker BR, Flier JS, Mullins JJ, Seckl JR 2004 Novel adipose tissue-mediated resistance to diet-induced visceral obesity in 11 β-hydroxysteroid dehydrogenase type 1-deficient mice. Diabetes 53:931–938
8. Seckl JR, Walker BR 2001 Minireview: 11β-hydroxysteroid dehydrogenase type 1—a tissue-specific amplifier of glucocorticoid action. Endocrinology 142:1371–1376
9. Bujalska IJ, Kumar S, Stewart PM 1997 Does central obesity reflect "Cushing's disease of the omentum"? Lancet 349:1210–1213
10. Wake DJ, Rask E, Livingstone DE, Soderberg S, Olsson T, Walker BR 2003 Local and systemic impact of transcriptional up-regulation of 11β-hydroxysteroid dehydrogenase type 1 in adipose tissue in human obesity. J Clin Endocrinol Metab 88:3983–3988
11. Alberts P, Nilsson C, Selen G, Engblom LO, Edling NH, Norling S, Klingstrom G, Larsson C, Forsgren M, Ashkzari M, Nilsson CE, Fiedler M, Bergqvist E, Ohman B, Bjorkstrand E, Abrahmsen LB 2003 Selective inhibition of 11 β-hydroxysteroid dehydrogenase type 1 improves hepatic insulin sensitivity in hyperglycemic mice strains. Endocrinology 144:4755–4762
12. Hermanowski-Vosatka A, Balkovec JM, Cheng K, Chen HY, Hernandez M, Koo GC, Le Grand CB, Li Z, Metzger JM, Mundt SS, Noonan H, Nunes CN, Olson SH, Pikounis B, Ren N, Robertson N, Schaeffer JM, Shah K, Springer MS, Strack AM, Strowski M, Wu K, Wu T, Xiao J, Zhang BB, Wright SD, Thieringer R 2005 11β-HSD1 inhibition ameliorates metabolic syndrome and prevents progression of atherosclerosis in mice. J Exp Med 202:517–527
13. Cinti S, Mitchell G, Barbatelli G, Murano I, Ceresi E, Faloia E, Wang S, Fortier M, Greenberg AS, Obin MS 2005 Adipocyte death defines macrophage localization and function in adipose tissue of obese mice and humans. J Lipid Res 46:2347–2355
14. Neels JG, Olefsky JM 2006 Inflamed fat: what starts the fire? J Clin Invest 116:33–35
15. Tchkonia T, Giorgadze N, Pirtskhalava T, Thomou T, DePonte M, Koo A, Forse RA, Chinnappan D, Martin-Ruiz C, von Zglinicki T, Kirkland JL 2006 Fat depot-specific characteristics are retained in strains derived from single human preadipocytes. Diabetes 55:2571–2578
16. Schaffler A, Scholmerich J, Buchler C 2005 Mechanisms of disease: adipocytokines and visceral adipose tissue—emerging role in intestinal and mesenteric diseases. Nat Clin Pract Gastroenterol Hepatol 2:103–111
17. Paulmyer-Lacroix O, Boullu S, Oliver C, Alessi MC, Grino M 2002 Expression of the mRNA coding for 11β-hydroxysteroid dehydrogenase type 1 in adipose tissue from obese patients: an in situ hybridization study. J Clin Endocrinol Metab 87:2701–2705
18. Mathias S, Pena LA, Kolesnick RN 1998 Signal transduction of stress via ceramide. Biochem J 335(Pt 3):465–480
19. Tani M, Ito M, Igarashi Y 2006 Ceramide/sphingosine/sphingosine 1-phosphate metabolism on the cell surface and in the extracellular space. Cell Signal 19:229–237
20. Minokoshi Y, Kim YB, Peroni OD, Fryer LG, Muller C, Carling D, Kahn BB 2002 Leptin stimulates fatty-acid oxidation by activating AMP-activated protein kinase. Nature 415:339–343
21. Hardie DG 2003 Minireview: the AMP-activated protein kinase cascade: the key sensor of cellular energy status. Endocrinology 144:5179–5183
22. Tanaka T, Hidaka S, Masuzaki H, Yasue S, Minokoshi Y, Ebihara K, Chusho H, Ogawa Y, Toyoda T, Sato K, Miyanaga F, Fujimoto M, Tomita T, Kusakabe T, Kobayashi N, Tanioka H, Hayashi T, Hosoda K, Yoshimatsu H, Sakata T, Nakao K 2005 Skeletal muscle AMP-activated protein kinase phosphorylation parallels metabolic phenotype in leptin transgenic mice under dietary modification. Diabetes 54:2365–2374
23. Dagon Y, Avraham Y, Berry EM 2006 AMPK activation regulates apoptosis, adipogenesis, and lipolysis by eIF2α in adipocytes. Biochem Biophys Res Commun 340:43–47
24. Gaidhu MP, Fediuc S, Ceddia RB 2006 5-Aminoimidazole-4-carboxamide-1-β-D-ribofuranoside-induced AMP-activated protein kinase phosphorylation inhibits basal and insulin-stimulated glucose uptake, lipid synthesis, and fatty acid oxidation in isolated rat adipocytes. J Biol Chem 281:25956–25964
25. Wang M, Crisostomo PR, Herring C, Meldrum KK, Meldrum DR 2006 Human progenitor cells from bone marrow or adipose tissue produce VEGF, HGF, and IGF-I in response to TNF by a p38 MAPK-dependent mechanism. Am J Physiol Regul Integr Comp Physiol 291:R880–R884
26. Benson SC, Pershadsingh HA, Ho CI, Chittiboyina A, Desai P, Pravenec M, Qi N, Wang J, Avery MA, Kurtz TW 2004 Identification of telmisartan as a unique angiotensin II receptor antagonist with selective PPARγ-modulating activity. Hypertension 43:993–1002
27. Fujimoto M, Masuzaki H, Tanaka T, Yasue S, Tomita T, Okazawa K, Fujikura J, Chusho H, Ebihara K, Hayashi T, Hosoda K, Nakao K 2004 An angiotensin II AT1 receptor antagonist, telmisartan augments glucose uptake and GLUT4 protein expression in 3T3-L1 adipocytes. FEBS Lett 576:492–497
28. Li J, Coven DL, Miller EJ, Hu X, Young ME, Carling D, Sinusas AJ, Young LH 2006 Activation of AMPK α- and γ-isoform complexes in the intact ischemic rat heart. Am J Physiol Heart Circ Physiol 291:H1927–H1934
29. Salt IP, Connell JM, Gould GW 2000 5-Aminoimidazole-4-carboxamide ribonucleoside (AICAR) inhibits insulin-stimulated glucose transport in 3T3-L1 adipocytes. Diabetes 49:1649–1656
30. Voice MW, Seckl JR, Chapman KE 1996 The sequence of 5′ flanking DNA from the mouse 11β-hydroxysteroid dehydrogenase type 1 gene and analysis of putative transcription factor binding sites. Gene 181:233–235
31. Smas CM, Sul HS 1993 Pref-1, a protein containing EGF-like repeats, inhibits adipocyte differentiation. Cell 73:725–734
32. Boney CM, Fiedorek Jr FT, Paul SR, Gruppuso PA 1996 Regulation of preadipocyte factor-1 gene expression during 3T3-L1 cell differentiation. Endocrinology 137:2923–2928
33. Wang E, Norred WP, Bacon CW, Riley RT, Merrill Jr AH 1991 Inhibition of sphingolipid biosynthesis by fumonisins. Implications for diseases associated with Fusarium moniliforme. J Biol Chem 266:14486–14490
34. Miyake Y, Kozutsumi Y, Nakamura S, Fujita T, Kawasaki T 1995 Serine palmitoyltransferase is the primary target of a sphingosine-like immunosuppressant, ISP-1/myriocin. Biochem Biophys Res Commun 211:396–403
35. Albouz S, Hauw JJ, Berwald-Netter Y, Boutry JM, Bourdon R, Baumann N 1981 Tricyclic antidepressants induce sphingomyelinase deficiency in fibroblast and neuroblastoma cell cultures. Biomedicine 35:218–220
36. McCormick KL, Wang X, Mick GJ 2006 Evidence that the 11 β-hydroxysteroid dehydrogenase (11 β-HSD1) is regulated by pentose pathway flux. Studies in rat adipocytes and microsomes. J Biol Chem 281:341–347
37. Corton JM, Gillespie JG, Hawley SA, Hardie DG 1995 5-Aminoimidazole-4-carboxamide ribonucleoside. A specific method for activating AMP-activated protein kinase in intact cells? Eur J Biochem 229:558–565
38. Zhou G, Myers R, Li Y, Chen Y, Shen X, Fenyk-Melody J, Wu M, Ventre J, Doebber T, Fujii N, Musi N, Hirshman MF, Goodyear LJ, Moller DE 2001 Role of AMP-activated protein kinase in mechanism of metformin action. J Clin Invest 108:1167–1174
39. Floyd ZE, Stephens JM 2003 STAT5A promotes adipogenesis in nonprecursor cells and associates with the glucocorticoid receptor during adipocyte differentiation. Diabetes 52:308–314
40. Williams LJ, Lyons V, MacLeod I, Rajan V, Darlington GJ, Poli V, Seckl JR, Chapman KE 2000 C/EBP regulates hepatic transcription of 11β-hydroxysteroid dehydrogenase type 1. A novel mechanism for cross-talk between the C/EBP and glucocorticoid signaling pathways. J Biol Chem 275:30232–30239
41. Tang QQ, Zhang JW, Lane DM 2004 Sequential gene promoter interactions of C/EBPβ, C/EBPα, and PPARγ during adipogenesis. Biochem Biophys Res Commun 319:235–239
42. Sawai H, Okazaki T, Yamamoto H, Okano H, Takeda Y, Tashima M, Sawada H, Okuma M, Ishikura H, Umehara H, Domae N 1995 Requirement of AP-1 for ceramide-induced apoptosis in human leukemia HL-60 cells. J Biol Chem 270:27326–27331
43. Summers SA, Nelson DH 2005 A role for sphingolipids in producing the common features of type 2 diabetes, metabolic syndrome X, and Cushing's syndrome. Diabetes 54:591–602
44. Chavez JA, Holland WL, Bar J, Sandhoff K, Summers SA 2005 Acid ceramidase overexpression prevents the inhibitory effects of saturated fatty acids on insulin signaling. J Biol Chem 280:20148–20153
45. Samad F, Hester KD, Yang G, Hannun YA, Bielawski J 2006 Altered adipose and plasma sphingolipid metabolism in obesity: a potential mechanism for cardiovascular and metabolic risk. Diabetes 55:2579–2587
46. Andrieu N, Salvayre R, Jaffrezou JP, Levade T 1995 Low temperatures and

hypertonicity do not block cytokine-induced stimulation of the sphingomyelin pathway but inhibit nuclear factor-κB activation. J Biol Chem 270:24518–24524
47. **Fain JN, Madan AK** 2005 Regulation of monocyte chemoattractant protein 1 (MCP-1) release by explants of human visceral adipose tissue. Int J Obes (Lond) 29:1299–1307
48. **Jun DJ, Lee JH, Choi BH, Koh TK, Ha DC, Jeong MW, Kim KT** 2006 Sphingosine-1-phosphate modulates both lipolysis and leptin production in differentiated rat white adipocytes. Endocrinology 147:5835–5844
49. **Hannun YA** 1996 Functions of ceramide in coordinating cellular responses to stress. Science 274:1855–1859
50. **Bielawska A, Linardic CM, Hannun YA** 1992 Modulation of cell growth and differentiation by ceramide. FEBS Lett 307:211–214
51. **Bose R, Verheij M, Haimovitz-Friedman A, Scotto K, Fuks Z, Kolesnick R** 1995 Ceramide synthase mediates daunorubicin-induced apoptosis: an alternative mechanism for generating death signals. Cell 82:405–414
52. **Verheij M, Bose R, Lin XH, Yao B, Jarvis WD, Grant S, Birrer MJ, Szabo E, Zon LI, Kyriakis JM, Haimovitz-Friedman A, Fuks Z, Kolesnick RN** 1996 Requirement for ceramide-initiated SAPK/JNK signalling in stress-induced apoptosis. Nature 380:75–79
53. **Gulbins E, Kolesnick R** 2003 Raft ceramide in molecular medicine. Oncogene 22:7070–7077
54. **Valerio A, Cardile A, Cozzi V, Bracale R, Tedesco L, Pisconti A, Palomba L, Cantoni O, Clementi E, Moncada S, Carruba MO, Nisoli E** 2006 TNF-α downregulates eNOS expression and mitochondrial biogenesis in fat and muscle of obese rodents. J Clin Invest 116:2791–2798
55. **Zhang JW, Klemm DJ, Vinson C, Lane MD** 2004 Role of CREB in transcriptional regulation of CCAAT/enhancer-binding protein β gene during adipogenesis. J Biol Chem 279:4471–4478
56. **Habinowski SA, Witters LA** 2001 The effects of AICAR on adipocyte differentiation of 3T3–L1 cells. Biochem Biophys Res Commun 286:852–856
57. **Newell FS, Su H, Tornqvist H, Whitehead JP, Prins JB, Hutley LJ** 2006 Characterization of the transcriptional and functional effects of fibroblast growth factor-1 on human preadipocyte differentiation. FASEB J 20:2615–2617
58. **Wang B, Trayhurn P** 2006 Acute and prolonged effects of TNF-α on the expression and secretion of inflammation-related adipokines by human adipocytes differentiated in culture. Pflugers Arch 452:418–427
59. **Tchoukalova YD, Sarr MG, Jensen MD** 2004 Measuring committed preadipocytes in human adipose tissue from severely obese patients by using adipocyte fatty acid binding protein. Am J Physiol Regul Integr Comp Physiol 287:R1132–R1140
60. **Tchoukalova Y, Koutsari C, Jensen M** 2007 Committed subcutaneous preadipocytes are reduced in human obesity. Diabetologia 50:151–157
61. **Ramji DP, Foka P** 2002 CCAAT/enhancer-binding proteins: structure, function and regulation. Biochem J 365:561–575
62. **Fujimoto M, Masuzaki H, Yamamoto Y, Norisada N, Imori M, Yoshimoto M, Tomita T, Tanaka T, Okazawa K, Fujikura J, Chusho H, Ebihara K, Hayashi T, Hosoda K, Inoue G, Nakao K** 2005 CCAAT/enhancer binding protein α maintains the ability of insulin-stimulated GLUT4 translocation in 3T3–C2 fibroblastic cells. Biochim Biophys Acta 1745:38–47
63. **Gout J, Tirard J, Thevenon C, Riou JP, Begeot M, Naville D** 2006 CCAAT/enhancer-binding proteins (C/EBPs) regulate the basal and cAMP-induced transcription of the human 11β-hydroxysteroid dehydrogenase encoding gene in adipose cells. Biochimie (Paris) 88:1115–1124

Endocrinology **is published monthly by The Endocrine Society (http://www.endo-society.org), the foremost professional society serving the endocrine community.**

Am J Physiol Endocrinol Metab 292: E1213–E1222, 2007.
First published December 26, 2006; doi:10.1152/ajpendo.00340.2006.

Bezafibrate regulates the expression and enzyme activity of 11β-hydroxysteroid dehydrogenase type 1 in murine adipose tissue and 3T3-L1 adipocytes

Shigeru Nakano,[1]* Yoichi Inada,[1]* Hiroaki Masuzaki,[2] Tomohiro Tanaka,[2] Shintaro Yasue,[2] Takako Ishii,[2] Naoki Arai,[2] Ken Ebihara,[2] Kiminori Hosoda,[2] Kazuyasu Maruyama,[1] Yoshinobu Yamazaki,[1] Nobuo Shibata,[3] and Kazuwa Nakao[2]

[1]*Pharmacology Research Laboratory R&D, and* [3]*Development Research Department R&D, Kissei Pharmaceutical, Nagano; and* [2]*Department of Medicine and Clinical Science, Kyoto University Graduate School of Medicine, Kyoto, Japan*

Submitted 13 July 2006; accepted in final form 20 December 2006

Nakano S, Inada Y, Masuzaki H, Tanaka T, Yasue S, Ishii T, Arai N, Ebihara K, Hosoda K, Maruyama K, Yamazaki Y, Shibata N, Nakao K. Bezafibrate regulates the expression and enzyme activity of 11β-hydroxysteroid dehydrogenase type 1 in murine adipose tissue and 3T3-L1 adipocytes. *Am J Physiol Endocrinol Metab* 292: E1213–E1222, 2007. First published December 26, 2006; doi:10.1152/ajpendo.00340.2006.—A clinically employed antihyperlipidemic drug, bezafibrate, has been characterized as a PPAR(α, -γ, and -δ) pan-agonist in vitro. Recent extended trials have highlighted its antidiabetic properties in humans. However, the underlying molecular mechanism is not fully elucidated. The present study was designed to explore potential regulatory mechanisms of intracellular glucocorticoid reactivating enzyme, 11β-HSD1 and anti-diabetic hormone, adiponectin by bezafibrate in murine adipose tissue, and cultured adipocytes. Treatment of *db/db* mice with bezafibrate significantly ameliorated hyperglycemia and insulin resistance, accompanied by a marked reduction of triglyceride and nonesterified fatty acids. Despite equipotent in lipid-lowering effects, another fibrate, fenofibrate, did not show such beneficial effects on glycemic control. Treatment of bezafibrate caused a marked decrease in the mRNA level of 11β-HSD1 preferentially in adipose tissue of *db/db* mice (−47%, $P < 0.05$), concomitant with a significant increase in plasma adiponectin level (+37%, $P < 0.01$). Notably, treatment of bezafibrate caused a marked decrease in the mRNA level (−34%, $P < 0.01$) and enzyme activity (−32%, $P < 0.01$) of 11β-HSD1, whereas the treatment substantially augmented the expression (+71%, $P < 0.01$) and secretion (+27%, $P < 0.01$) of adiponectin in 3T3-L1 adipocytes. Knockdown of 11β-HSD1 by siRNA confirmed that 11β-HSD1 acts as a distinct oxoreductase in adipocytes and validated the enzyme activity assays in the present study. Effects of bezafibrate on regulation of 11β-HSD1 and adiponectin in murine adipocytes were comparable with those in thiazolidinediones. This is the first demonstration that bezafibrate directly regulates 11β-HSD1 and adiponectin in murine adipocytes, both of which may contribute to metabolically-beneficial effects by bezafibrate.

metabolic syndrome; adiponectin

FAMILY GENES of peroxisome proliferator-activated receptors (PPARs) are profoundly relevant to fuel homeostasis (14, 41). Agonists for PPARα and PPARγ have been widely used for the treatment of dyslipidemia and type 2 diabetes (46). Recent research progress (3) has highlighted the potential usefulness of PPARα/γ dual agonists or PPAR(α, -γ, and -δ) pan-agonists for metabolic diseases. However, some of these compounds are reported to cause adverse effects, including carcinogenesis, edema, hepatotoxicity, and increase in body weight in rodent experiments (45). Bezafibrate has been widely used for the treatment of dyslipidemia in human clinics (11). Recent in vitro experiments have shown that bezafibrate serves as a pan-agonist for PPARα, -γ, and -δ (9, 48). Furthermore, recent extended clinical trials (15, 43) have highlighted its antidiabetic properties. However, the underlying mechanism is not fully clarified. To explore unidentified mechanisms whereby bezafibrate ameliorates metabolic derangement, using genetically obese diabetic BKS.Cg-+Lepr^{db}/+Lept^{db} (*db/db*) mice, which represent a cluster of detrimental metabolic sequelae such as morbid obesity, diabetes, dyslipidemia, and liver steatosis (39), we examined metabolic response to bezafibrate.

Intracellular glucocorticoid reactivating enzyme 11β-hydroxysteroid dehydrogenase type 1 (11β-HSD1) is abundantly expressed in liver, adipose tissue, skeletal muscle, and central nervous system (38). Targeted overexpression of 11β-HSD1 in adipose tissue in mice results in visceral fat obesity, insulin resistance, and hypertension, suggesting that increased level of adipose 11β-HSD1 plays a critical role in metabolic derangements by providing local glucocorticoid excess within fat cells (29, 30). On the other hand, 11β-HSD1 knockout mice (32), as well as adipose-specific 11β-HSD2 overexpressors, which mimicked adipose-specific 11β-HSD1 knockout mice (18), are protected against the metabolic syndrome under overnutrition. Furthermore, recent studies (36, 47) in rodents suggest that local glucocorticoid excess mediated by 11β-HSD1 in liver or skeletal muscle is also involved in the pathophysiology of the metabolic diseases.

Here, we show that bezafibrate potently decreases the mRNA level of 11β-HSD1 (28) in adipose tissue of *db/db* mice. We also demonstrate for the first time that bezafibrate inhibits the expression and enzyme activity of 11β-HSD1 in 3T3-L1 adipocytes. Our data show that bezafibrate potently increases the plasma level of antidiabetic adiponectin (26) in mice and augments substantially the expression and secretion of adiponectin in 3T3-L1 adipocytes. To our knowledge, this is the first study to demonstrate that bezafibrate potently regulates 11β-HSD1 and adiponectin in murine fat cells.

* Shigeru Nakano and Yoichi Inada contributed equally to this work.

Address for reprint requests and other correspondence: H. Masuzaki, Dept. of Medicine and Clinical Science, Kyoto University Graduate School of Medicine, 54 Shogoin-Kawaharacho, Sakyo-ku, Kyoto, 606-8507, Japan (e-mail: hiroaki@kuhp.kyoto-u.ac.jp).

The costs of publication of this article were defrayed in part by the payment of page charges. The article must therefore be hereby marked "*advertisement*" in accordance with 18 U.S.C. Section 1734 solely to indicate this fact.

MATERIALS AND METHODS

Materials. Bezafibrate was obtained from Chugai Pharmaceutical (Tokyo, Japan). Fenofibrate and WY-14,643 were purchased from Sigma-Aldrich (St. Louis, MO). Pioglitazone hydrochloride (pioglitazone), fenofibric acid, an active metabolite of fenofibrate, and rosiglitazone were synthesized by Kissei Pharmaceutical (Matsumoto, Japan). WY-14,643 and fenofibric acid were used for in vitro experiments.

Animal experiments. Animal experiments in the present study were conducted in accordance with the guidelines for animal experiments of Kissei Pharmaceutical and the Animal Research Committee, Graduate School of Medicine, Kyoto University, and were approved by the Japanese Pharmacological Society. Six-week-old male BKS.Cg-m+/+Lept^{db}/Jcl (lean) mice and their obese littermates, BKS.Cg-+Lepr^{db}/+Lept^{db}/Jcl (*db/db*) mice, were purchased from Clea Japan (Tokyo, Japan). Mice were housed individually with free access to tap water and commercial pellet food (CE-2; Clea Japan) and kept at 23°C with a humidity of 55% under a 12:12-h light-dark cycle. Mice were randomly divided into groups before each experiment. Bezafibrate (100 or 300 mg·kg^{-1}·day^{-1}), fenofibrate (300 mg·kg^{-1}·day^{-1}), pioglitazone (30 mg·kg^{-1}·day^{-1}), rosiglitazone (10 mg·kg^{-1}·day^{-1}), or vehicle (1% methylcellulose) were orally administered to *db/db* mice once per day at ~10:00 AM for 6 or 8 wk. Simultaneously, vehicle was administered to lean mice for 6 or 8 wk. Body weight and food consumption were monitored twice per week.

Measurement of metabolic parameters in plasma. Blood samples were collected from tail vein with heparinized hematocrit tube into the collection tube with 50 U aprotinin (Trasylol; Bayer Yakuhin, Osaka, Japan) when fed ad libitum at around 10:00 AM. Plasma glucose, triglyceride (TG), and nonesterified fatty acids (NEFA) were measured via commercially-available kits (Glucose CII-test, Triglyceride E-test, and NEFA C test, respectively; Wako Pure Chemical Industries, Osaka, Japan). Plasma LDL cholesterol and HDL cholesterol were measured by Cholestest LDL and Cholestest N HDL (Daiichi Pure Chemicals, Tokyo, Japan) with a biochemistry automatic analyzer (Clinical analyzer 7150; Hitachi High-Technologies, Tokyo, Japan). Plasma insulin, leptin, adiponectin, and corticosterone concentrations were determined using Insulin ELISA kit, Mouse Leptin ELISA kit (Morinaga Institute of Biological Science, Yokohama, Japan), Mouse/Rat Adiponectin ELISA Kit (Otsuka Pharmaceutical, Tokushima, Japan), and AssayMax Corticosterone ELISA kit (Assay-Pro, Winfield, MO), respectively.

Oral glucose tolerance test. At 4 wk after the treatments were initiated, *db/db* and lean mice fasted for 12 h were orally administered 2 g/kg body wt glucose (Wako Pure Chemical Industries). Blood sample was collected from tail vein at 0.5, 1, 1.5, and 2 h after glucose load. The areas under the curve (AUC) of glucose levels (0–0.5 and 0–1 h) were calculated to assess the status of glucose homeostasis by the linear trapezoidal equation (35).

Intravenous insulin tolerance test. At 2 wk after the treatments were initiated, *db/db* and lean mice fasted for 12 h were injected 0.8 U/kg body wt insulin (Novo Nordisk Pharma, Tokyo, Japan) via the tail vein. Blood was collected from tail vein at 0.5, 1, 1.5, and 2 h after insulin injection. The AUC of glucose levels (0–0.5 and 0–1 h) were calculated to assess the status of insulin resistance by the equation described above.

TG and total cholesterol contents in liver. At 8 wk after the treatments were initiated, mice were anesthetized with intraperitonial injection of 20% chloral hydrate (Wako Pure Chemical Industries). Removed liver tissue was quickly weighed, and one part was homogenized and subjected to lipid extraction according to the method of Folch et al. (7). Hepatic TG and cholesterol contents were measured using commercially available kits (TG E-test and cholesterol E-test; Wako Pure Chemical Industries).

Determination of mRNA levels. Total RNA was isolated from liver, mesenteric fat, subcutaneous fat, triceps surae muscle, and 3T3-L1 adipocytes by Isogen (Nippon Gene, Tokyo, Japan). The mRNA level corresponding to a couple of target genes was determined by real-time quantitative RT-PCR using a GeneAmp 5700 Sequence Detection System (Applied Biosystems, Foster City, CA). Primers and double-dye probes for carnitine palmitoyltransferase (CPT) I, acyl-CoA oxidase (ACO), uncoupling protein (UCP)3, and adiponectin were designed using Primer Express 2.0 (Applied Biosystems; Table 1). Primers and double-dye probes for 11β-HSD1 and UCP2 were designed as described previously (1, 16). Results were normalized to 18S ribosomal RNA concentration determined by PreDeveloped TaqMan Assay Reagents (Applied Biosystems).

Cell culture and treatment. 3T3-L1 preadipocytes (passages 3–10; American Type Culture Collection, Manassas, VA) were grown and differentiated into adipocytes, as described previously (8). Briefly, differentiation was induced by incubating the cells in DMEM that included 10% FBS with 0.5 mmol/l IBMX, 1 μmol/l dexamethazone, and 10 μg/ml insulin for 2 days, followed by another 2-day incubation in DMEM that included 10% FBS with 10 μg/ml insulin. The cells were further incubated in DMEM with 10% FBS for an additional 4 days to complete the adipocyte conversion. At *day 8* following the initiation of differentiation, vehicle (1% DMSO), bezafibrate (1–300 μmol/l), rosiglitazone (3 μmol/l), pioglitazone (10 μmol/l), fenofibric acid (1–300 μmol/l), or WY-14,643 (1–10 μmol/l) were replenished to cultured cells and coincubated from 8 to 48 h at 37°C in 5% CO_2.

Table 1. *Primers and double-dye probes used for real-time quantitative PCR*

Name	Oligonucleotide Sequence	Amplicon Size, bp	Accession No.
ACO			
Forward:	5′-TGCACCCGCCCATGAC-3′	72	AF006688
Reverse:	5′-GGCAACGGCCGAAAGC-3′		
Probe:	FAM5′-TCCTGACACAGCTAAGTTGCTTGTCTTTACCTCC-3′ TAM		
CPT I			
Forward:	5′-CCTCCCTGGGCATGATTG-3′	87	AF017175
Reverse:	5′-ACGCCACTCACGATGTTCTTC-3′		
Probe:	FAM5′-CACCACTGGCCGCATGTCAAGC-3′ TAM		
UCP3			
Forward:	5′-TGGCCCAACATCACAAGAAA-3′	79	NM_009464
Reverse:	5′-TCCAGCAACTTCTCCTTGATGA-3′		
Probe:	FAM5′-TGTCAACTGTGCTGAGATGGTGACCTACGA-3′ TAM		
Adiponectin			
Forward:	5′-CAGTGGATCTGACGACAC-3′	74	U37222
Reverse:	5′-TGGGCAGGATTAAGAGGAACA-3′		
Probe:	FAM5′-AGGGCTCAGGATGCTACTGTTGCAAGCT-3′ TAM		

ACO, acyl-CoA oxidase; CPT I, carnitine palmitoyltransferase I; UCP3, uncoupling protein 3.

Suppression of 11β-HSD1 expression by RNA interference. 11β-HSD1 expression in 3T3-L1 differentiated adipocytes was suppressed by a small interfering RNA (siRNA) duplex oligonucleotide-targeted 11β-HSD1 mRNA sequence. Individual siRNA duplex was designed using a siRNA Design Support System (TaKaRa Bio, Shiga, Japan). 3T3-L1 differentiated adipocytes (*day 8*) were transfected with the siRNA duplex (10 nmol/l; sense: 5′-GAAAUGGCAUAUCAUCUGUTT-3′ and antisense: 3′-TTCUUUACCGUAUAGUAGACA-5′) using *Trans*IT-TKO Transfection Reagent (Mirus Bio, Madison, WI) for 48 h. Negative Control siRNA (Qiagen, Tokyo, Japan) was used as a nonsilencing control.

Measurement of 11β-HSD1 enzyme activity. Oxoreductase enzyme activity of 11β-HSD1 was assessed according to a previous report (5), with slight modification. Assays for 11β-HSD1 activity were performed by incubating intact cells with corticosteroids with appropriate tritiated tracer. In assays for oxoreductase activity, cells were incubated in serum-free DMEM containing 250 nmol/l cortisone with appropriate tritium-labeled tracer [1,2-$^3H_2$]cortisone (50 Ci/mmol; American Radiolabeled Chemicals, St. Louis, MO). After the incubation at 37°C for indicated time, corticosteroids were extracted using ethyl acetate, separated by thin layer chromatography (TLC) in chloroform-methanol (95:5), and quantified by autoradiography. 11β-HSD1 oxoreductase activities were expressed as pmol product ([1,2-$^3H_2$]cortisol)·min^{-1}·well^{-1} after correction for apparent conversion in reactions without cells.

Western blot analysis. 3T3-L1 pre- or differentiated adipocytes were coincubated with drugs or vehicle for 24 h. Proteins in cultured media (25 ng/lane) were separated by standard Laemmli's method (23) and subjected to immunoblotting. Western blot analyses were performed using anti-mouse adiponectin antibody (MAB3608; Chemicon International, Temecula, CA).

Statistical analyses. All data were expressed as means ± SE. All statistical analyses were performed using SAS System Version 8.2 (SAS Institute, Cary, NC) and its interlocking movement program, Clinical Package Version 5.0. Student's *t*-test was performed between *1*) vehicle-treated lean mice and vehicle-treated *db/db* mice, *2*) vehicle-treated 3T3-L1 differentiated adipocytes and vehicle-treated 3T3-L1 preadipocytes, and *3*) nontransfected control and nonsilencing control or siRNA transfected for RNA interference experiments. In case of multiple comparisons, one-way analysis of variance (ANOVA) followed by post hoc analysis of Dunnett's multiple comparison test was performed. Statistical analysis between vehicle-treated *db/db* mice and other groups in oral glucose tolerance test (OGTT) and intravenous insulin tolerance test (IVITT) were performed using Student's *t*-test or Dunnett's multiple comparison test, followed by univariate repeated-measures ANOVA, taking pretreatment values as covariate. Differences were considered significant at $P < 0.05$.

RESULTS

Body weight and food consumption. Increment in body weight and food consumption in *db/db* mice was exaggerated compared with lean mice during the course of the experiment ($P < 0.01$). Both bezafibrate and fenofibrate tended to increase body weight compared with vehicle-treated *db/db* mice ($P = 0.055$ by ANOVA; Table 2).

Liver and mesenteric fat weight. Liver and mesenteric fat weight in vehicle-treated *db/db* mice was significantly elevated compared with vehicle-treated lean mice ($P < 0.01$; Table 2). Treatments of both bezafibrate and fenofibrate significantly increased liver weight compared with vehicle-treated *db/db* mice, whereas increase in liver weight in fenofibrate treatment was exaggerated compared with that in bezafibrate treatment (Table 2). It should be noted that both treatments did not significantly increase mesenteric fat weight ($P = 0.63$ by ANOVA; Table 2).

Plasma lipid parameters. Plasma levels of TG, NEFA, HDL cholesterol, and LDL cholesterol in vehicle-treated *db/db* mice at 15 wk of age were significantly higher than those in vehicle-treated lean mice ($P < 0.01$; Table 2). Both bezafibrate and fenofibrate markedly lowered plasma TG levels to around normal range at 8 wk after the treatments were initiated (Table 2). In addition, both treatments significantly lowered plasma level of NEFA (Table 2). Furthermore, both compounds significantly increased HDL cholesterol level in plasma (Table 2). In contrast, both compounds did not alter LDL cholesterol level in plasma (Table 2).

Hepatic TG and total cholesterol contents. Hepatic TG content in vehicle-treated *db/db* mice at 15 wk of age was significantly higher than that in vehicle-treated lean mice ($P <$

Table 2. *Body weight, food consumption, liver weight, mesenteric fat weight, plasma lipid level, and hepatic lipid content in db/db and vehicle-treated lean mice*

			Bezafibrate		Fenofibrate
	Lean	Vehicle	100	300	300
		Physical parameters			
Body weight, g (15 wk of age)	29±0.7##	34±1	39±1	38±3	41±1
Average food consumption, g (7–15 wk of age)	5.1±0.2##	7.9±0.1	7.7±0.1	7.1±0.1	7.0±0.1
Liver weight, g	1.7±0.1##	2.3±0.1	3.3±0.1**	3.7±0.4**	4.8±0.1**
Mesenteric fat weight, mg	264±29##	598±70	771±91	729±160	738±71
		Plasma lipid parameters			
Triglyceride, mg/dl	113±10##	346±35	201±9**	135±15**	119±12**
NEFA, mEq/l	0.7±0.1##	2.1±0.2	1.4±0.2*	1.4±0.2*	1.3±0.2**
HDL cholesterol, mg/dl	40±2##	76±5	96±4**	98±6**	94±4*
LDL cholesterol, mg/dl	8±0##	15±1	14±2	14±2	14±1
		Hepatic lipid contents			
Triglyceride, mg/g liver	4.9±0.8##	12.2±0.7	10.3±0.4	8.4±0.5*	8.6±1.4*
Total cholesterol, mg/g liver	1.2±0.2	1.6±0.1	1.1±0.1**	0.9±0.1**	0.9±0.2**

Data are presented as means ± SE (n = 7–8 in each). Values for bezafibrate and fenofibrate are given in mg·kg^{-1}·day^{-1}. NEFA, nonesterified fatty acids. ##$P < 0.01$ vs. vehicle-treated *db/db* mice (Student's *t*-test). *$P < 0.05$; **$P < 0.01$ vs. vehicle-treated *db/db* mice (1 way ANOVA followed by Dunnett's multiple comparison test).

0.01; Table 2). Bezafibrate and fenofibrate significantly reduced hepatic TG and total cholesterol contents compared with vehicle-treated *db/db* mice (Table 2).

Plasma glucose and insulin levels. Plasma glucose levels in vehicle-treated *db/db* mice at 15 wk of age were significantly higher than those in vehicle-treated lean mice ($P < 0.01$; Fig. 1*A*). Bezafibrate significantly reduced plasma glucose levels at 8 wk after the treatments were initiated. In contrast, fenofibrate did not show beneficial effects on plasma glucose levels (Fig. 1*A*). Plasma insulin levels in vehicle-treated *db/db* mice at 15 wk of age tended to be higher than those in vehicle-treated lean mice ($P = 0.12$; Fig. 1*B*). Both bezafibrate and fenofibrate showed a trend toward reducing plasma insulin levels at 8 wk after the treatments were initiated ($P = 0.78$ by ANOVA; Fig. 1*B*).

OGTT and IVITT. To further assess the potential impact of drug administration on glucose tolerance and insulin sensitivity, OGTT and IVITT were performed in *db/db* mice and lean mice. At 4 wk after the treatments were initiated, bezafibrate, pioglitazone, and rosiglitazone significantly lowered plasma glucose levels compared with vehicle-treated *db/db* mice, but not fenofibrate (bezafibrate: 117 ± 21 mg/dl, $P = 0.0004$; fenofibrate: 197 ± 23 mg/dl, $P = 0.24$; pioglitazone: 143 ± 21 mg/dl, $P = 0.006$; rosiglitazone: 147 ± 27 mg/dl, $P = 0.007$ vs. vehicle-treated *db/db* mice; Fig. 2*A*). Glucose levels at each time point were significantly elevated in vehicle-treated *db/db* mice compared with vehicle-treated lean mice (Fig. 2*A*). $AUC_{0-0.5\ h}$ and $AUC_{0-1\ h}$ in vehicle-treated *db/db* mice were significantly higher than those in vehicle-treated lean mice (Table 3). Bezafibrate, pioglitazone, rosiglitazone and fenofibrate significantly reduced $AUC_{0-0.5\ h}$ and $AUC_{0-1\ h}$ (Table 3). Reduction of $AUC_{0-0.5\ h}$ and $AUC_{0-1\ h}$ in bezafibrate was exaggerated compared with fenofibrate.

At 2 wk after the treatments were initiated, bezafibrate and rosiglitazone significantly lowered plasma glucose levels compared with vehicle-treated *db/db* mice, but not pioglitazone and fenofibrate (bezafibrate: 197 ± 22 mg/dl, $P = 0.005$; fenofibrate: 253 ± 21 mg/dl, $P = 0.20$; pioglitazone: 258 ± 35 mg/dl, $P = 0.31$; rosiglitazone: 216 ± 28 mg/dl, $P = 0.021$ vs. vehicle-treated *db/db* mice; Fig. 2*B*). At 0.5 h after the insulin injection in IVITT, bezafibrate, pioglitazone, and rosiglitazone significantly reduced plasma glucose levels ($P < 0.05$). On the other hand, glucose-lowering effects in fenofibrate-treated mice were marginal ($P = 0.29$; Fig. 2*B*). $AUC_{0-0.5\ h}$ and $AUC_{0-1\ h}$ in vehicle-treated *db/db* mice were significantly higher than those in vehicle-treated lean mice (Table 3). Bezafibrate, pioglitazone, and rosiglitazone significantly reduced the value of $AUC_{0-0.5\ h}$, and reduction of $AUC_{0-1\ h}$ in bezafibrate was equipotent to rosiglitazone (Table 3). In contrast, fenofibrate represented no significant effects on AUCs.

Plasma leptin, adiponectin, and corticosterone levels. Plasma leptin levels in vehicle-treated *db/db* mice were markedly elevated compared with vehicle-treated lean mice ($P < 0.01$). Treatments of bezafibrate and fenofibrate did not change plasma leptin levels significantly in *db/db* mice ($P = 0.08$ by ANOVA), whereas pioglitazone significantly decreased the levels (Fig. 1*C*).

Plasma adiponectin levels in vehicle-treated *db/db* mice were significantly lower than those in vehicle-treated lean mice ($P < 0.01$; Fig. 1*D*). Treatments of bezafibrate, pioglitazone, and rosiglitazone caused a significant rise in plasma adiponec-

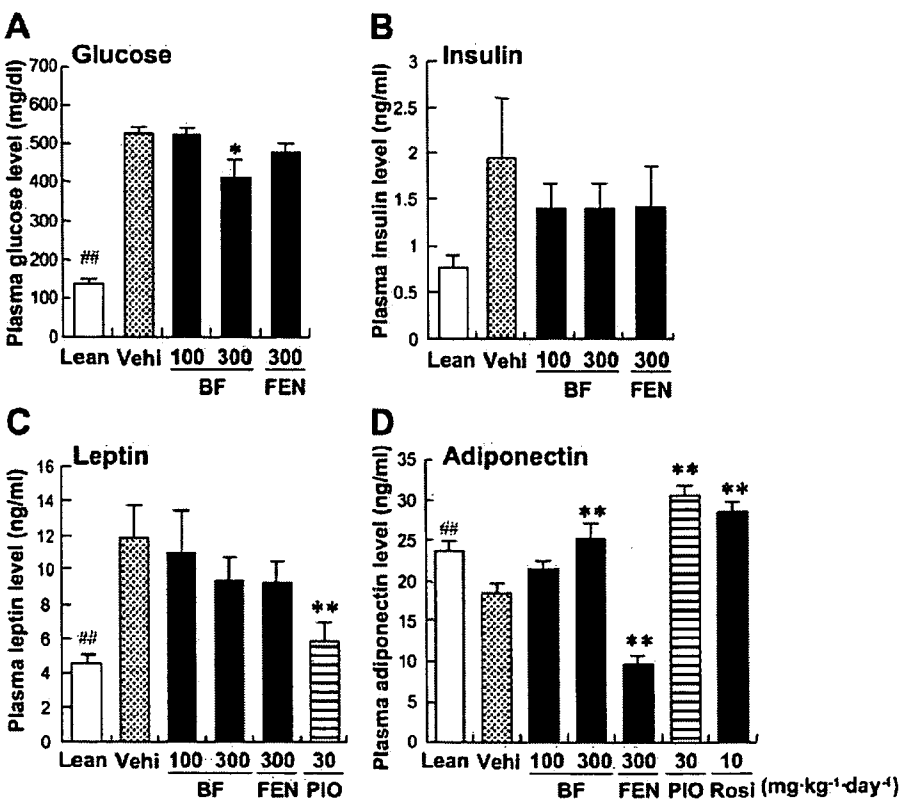

Fig. 1. Plasma glucose (*A*), plasma insulin (*B*), plasma leptin (*C*), and plasma adiponectin levels (*D*) in *db/db* mice treated with bezafibrate (BF; 100 or 300 mg·kg^{-1}·day^{-1}), fenofibrate (FEN; 300 mg·kg^{-1}·day^{-1}), pioglitazone (PIO; 30 mg·kg^{-1}·day^{-1}), rosiglitazone (Rosi; 10 mg·kg^{-1}·day^{-1}), or vehicle (Vehi) and vehicle-treated lean mice (n = 7–8 in each). Each column shows plasma glucose, insulin, and leptin levels at 8 wk and adiponectin levels in mice at 6 wk after the treatments were initiated. Data are presented as means ± SE. *$P < 0.05$; **$P < 0.01$ vs. vehicle-treated *db/db* mice; ##$P < 0.01$ vs. vehicle-treated *db/db* mice.

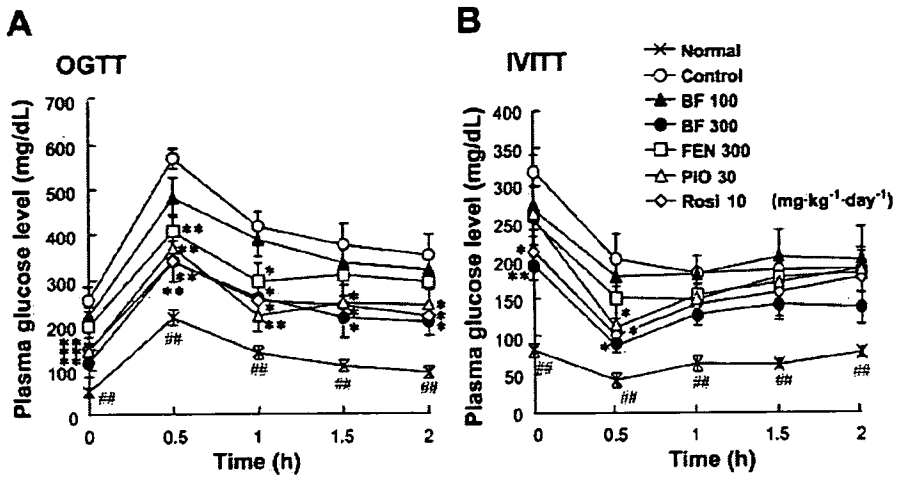

Fig. 2. Oral glucose tolerance test (OGTT; *A*) and intravenous insulin tolerance test (IVITT; *B*) in *db/db* mice treated with BF [100 (▲) or 300 mg·kg^{-1}·day^{-1}(●)], FEN [300 mg·kg^{-1}·day^{-1} (□)], PIO [30 mg·kg^{-1}·day^{-1}(△)], Rosi [10 mg·kg^{-1}·day^{-1} (◇)], or vehicle (○) and vehicle-treated lean mice (×) at 4 or 2 wk after initiating the treatments, respectively (n = 8–10 in each). Data of plasma glucose levels are presented as means ± SE. *P < 0.05; **P < 0.01 vs. vehicle-treated *db/db* analyzed by univariate repeated-measures ANOVA; ##P < 0.01 vs. vehicle-treated *db/db* mice.

tin levels. Conversely, fenofibrate rather decreased the levels compared with vehicle-treated *db/db* mice (Fig. 1*D*).

Plasma corticosterone level in vehicle-treated *db/db* mice (133.7 ± 21.3 ng/ml) was markedly elevated compared with vehicle-treated lean mice (37.4 ± 14.5 ng/ml, P < 0.01). Treatments of bezafibrate, fenofibrate, and pioglitazone did not significantly change plasma corticosterone levels in *db/db* mice (bezafibrate: 122.7 ± 14.2 ng/ml; fenofibrate: 121.2 ± 8.5 ng/ml; pioglitazone: 132.6 ± 14.7 ng/ml).

Expression of genes related to fuel metabolism in liver. It is well known (2) that the activation of PPARα induces mRNA expression of a series of genes involved in lipid handling and fatty acid β-oxidation. In liver, there were no significant differences in mRNA level of CPT I, ACO, UCP2, or UCP3 between vehicle-treated *db/db* and vehicle-treated lean mice (Table 4). On the other hand, both bezafibrate and fenofibrate markedly increased the levels for CPT I (P = 0.30 by ANOVA), ACO, UCP2, and UCP3 (bezafibrate, P = 0.23) compared with vehicle-treated *db/db* mice (Table 4).

Expression of 11β-HSD1 mRNA. In liver, triceps surae muscle, mesenteric fat, and subcutaneous fat, 11β-HSD1 mRNA levels in vehicle-treated *db/db* mice were significantly higher than those in vehicle-treated lean mice (Fig. 3). In liver, bezafibrate, fenofibrate, and pioglitazone significantly decreased the 11β-HSD1 mRNA levels (Fig. 3*A*). In triceps surae muscle, bezafibrate and fenofibrate also showed a trend toward a decrease in the 11β-HSD1 mRNA levels, but these effects were marginal (Fig. 3*A*).

Of note, in mesenteric fat, bezafibrate and pioglitazone substantially decreased the 11β-HSD1 expression levels, whereas fenofibrate did not affect the levels (Fig. 3*B*). In subcutaneous fat, bezafibrate also showed a trend toward lower levels of 11β-HSD1, which were comparable to those in pioglitazone. In contrast, fenofibrate had no effects (Fig. 3*B*).

mRNA expression levels and enzyme activity of 11β-HSD1 in bezafibrate-treated 3T3-L1 adipocytes. The mRNA levels of 11β-HSD1 in 3T3-L1 differentiated adipocytes were apparently higher than those in vehicle-treated 3T3-L1 preadipocytes. Importantly, bezafibrate, rosiglitazone, and pioglitazone markedly reduced the 11β-HSD1 mRNA levels in 3T3-L1 differentiated adipocytes at 48 h after the treatments. In contrast, fenofibrate and WY-14,643 had no effect on 11β-HSD1 mRNA levels (Fig. 4*A*).

To further explore the impact on enzyme activity of 11β-HSD1, cells were incubated with tritium-labeled cortisone. Assay for 11β-HSD1 activity clearly showed that 11β-HSD1 acted as distinct oxoreductase in 3T3-L1 differentiated adipocytes (Vehi; Fig. 4*B*). Bezafibrate, rosiglitazone, and pioglitazone considerably inhibited cortisone-to-cortisol conversion for 48-h treatment (Fig. 4*B*). Actually, bezafibrate, rosiglitazone, and pioglitazone markedly reduced 11β-HSD1 oxoreductase ac-

Table 3. *Effects of bezafibrate, fenofibrate, pioglitazone, rosiglitazone, or vehicle on AUC of plasma glusoce level in OGTT or IVITT*

Dose, mg·kg^{-1}·day^{-1}	OGTT		IVITT	
	$AUC_{0-0.5\,h}$	$AUC_{0-1\,h}$	$AUC_{0-0.5\,h}$	$AUC_{0-1\,h}$ (mg·h·dl^{-1})
Lean	68±4##	246±17##	32±3##	87±11##
Vehicle	207±7	702±28	131±13	228±24
Bezafibrate 100	176±14	612±53*	113±13	204±26
Bezafibrate 300	115±15**	415±59**	72±7**	127±12*
Fenofibrate 300	152±14*	504±48*	102±11	178±21
Pioglitazone 30	128±11**	424±38**	93±12*	160±20
Rosiglitazone 10	122±15**	420±59**	80±11**	127±23*

Data are presented as means ± SE (n = 8–10 in each). OGTT, oral glucose tolerance test; IVITT, introvenous insulin tolerance test. ##P < 0.01 vs. vehicle-treated *db/db* mice (Student's t-test); *P < 0.05; **P < 0.01 vs. vehicle-treated *db/db* mice (1-way ANOVA followed by Dunnett's multiple comparison test).

Table 4. *Hepatic mRNA levels related to fuel metabolism in db/db and vehicle-treated lean mice*

	Lean	Vehicle	Bezafibrate 100	Bezafibrate 300	Fenofibrate 300
CPT I	72±5	100±22	125±16	149±30	152±17
ACO	88±12	100±18	227±29*	279±26**	401±48**
UCP2	79±5	100±7	181±19	250±28**	352±51**
UCP3	203±73	100±26	1,273±380	3,782±2,639	7,777±1,441**

Data are presented as means ± SE (n = 7–8 in each). Values for bezafibrate and fenofibrate are given in mg·kg^{-1}·day^{-1}. *P < 0.05; **P < 0.01 vs. vehicle-treated *db/db* mice (1-way ANOVA followed by Dunnett's multiple comparison test).

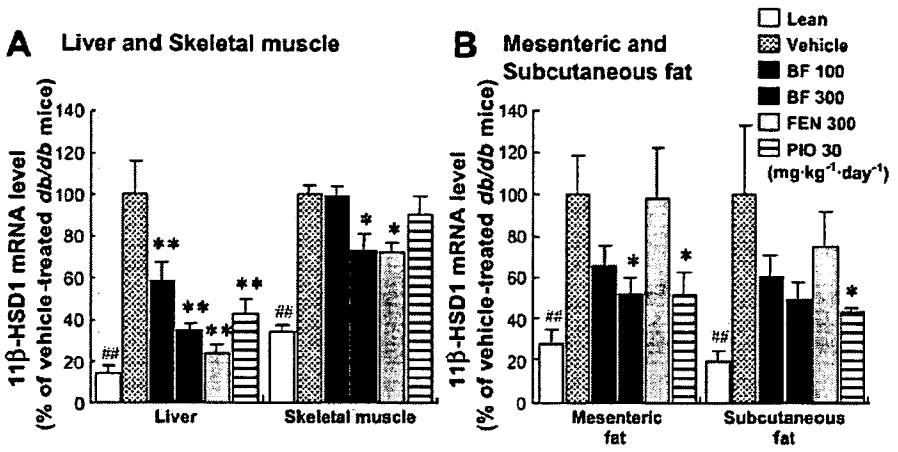

Fig. 3. 11β-hydroxysteroid dehydrogenase type 1 (11β-HSD1) mRNA levels in insulin target tissues of *db/db* mice treated with BF (100 or 300 mg·kg^{-1}·day^{-1}), FEN (300 mg·kg^{-1}·day^{-1}), PIO (30 mg·kg^{-1}·day^{-1}), or vehicle and vehicle-treated lean mice (n = 8–10 in each). Each column shows 11β-HSD1 mRNA levels in liver, triceps surae muscle (skeletal muscle; *A*), mesenteric fat, and subcutaneous fat (*B*) at 8 wk after the treatments were initiated. Each column represents %11β-HSD1 mRNA levels compared with vehicle-treated *db/db* mice (defined as 100%). Data are presented as means ± SE. *P < 0.05; **P < 0.01 vs. vehicle-treated *db/db* mice; ##P < 0.01 vs. vehicle-treated *db/db* mice.

tivities expressed as pmol product ([^{3}H]cortisol)·min^{-1}·well^{-1} (Fig. 4*C*).

Suppression of 11β-HSD1 expression and enzyme activity by transfection with a siRNA duplex. To validate the enzyme activity assay in the present study, 3T3-L1 differentiated adipocytes were transfected with siRNA duplex targeted to 11β-HSD1 mRNA sequence. The mRNA levels of 11β-HSD1 were markedly reduced by transfection of siRNA duplex (P < 0.01; Fig. 4*D*). Consequently, the enzyme activity of 11β-HSD1 was also reduced (P < 0.05; Fig. 4*E*).

Adiponectin level in cultured media of bezafibrate-treated 3T3-L1 adipocytes. Adiponectin levels in cultured media of 3T3-L1 adipocytes were determined by Western blot analysis. Adiponectin protein was detected as a single band at ~35 kDa (Fig. 5*A*). Adiponectin protein from vehicle-treated 3T3-L1 preadipocytes was under detectable range. Of note, bezafibrate and rosiglitazone markedly increased adiponectin level in cultured media. In contrast, adiponectin levels in media of cells treated with fenofibric acid did not increase at all (Fig. 5*B*).

The mRNA levels of adiponectin in 3T3-L1 adipocytes were determined at the point of 8, 16, and 24 h after the each treatment. Bezafibrate and rosiglitazone increased mRNA levels of adiponectin from 8 to 24 h in a time-dependent manner, with significant increases at 16 and 24 h (Fig. 5*C*). Consequently, at 24 h after the treatment, bezafibrate, rosiglitazone, and pioglitazone significantly increased the adiponectin mRNA levels (Fig. 5*D*).

DISCUSSION

Recent extensive clinical trials (43) provided compelling evidence that bezafibrate reduces the incidence of type 2 diabetes in patients with coronary artery diseases. To our knowledge, however, the underlying molecular mechanism of its metabolically beneficial effects has not been fully elucidated. The present study confirmed that repeated administration of bezafibrate significantly ameliorated hyperglycemia and insulin resistance in *db/db* mice. Nevertheless, antihyperlipidemic effects of fenofibrate were equipotent to bezafibrate (Table 2), and improvement of glucose homeostasis by fenofibrate was marginal compared with bezafibrate. In the present study, 100 or 300 mg·kg^{-1}·day^{-1} of bezafibrate and 300 mg·kg^{-1}·day^{-1} of fenofibrate were administered. Because the sensitivity of PPARα agonists in terms of fuel homeostasis in rodents is known to be much lower than in humans, higher doses have been commonly used for rodent experiments (12, 22, 49). Administered doses of compounds were decided mainly on the basis of their plasma TG-lowering effects. In our pilot study, treatment of bezafibrate or fenofibrate (100 mg·kg^{-1}·day^{-1}) in *db/db* mice for 8 wk did not significantly lower plasma levels of TG. In the next pilot study, treatment of bezafibrate (300 mg·kg^{-1}·day^{-1}) or fenofibrate (300 mg·kg^{-1}·day^{-1}) in *db/db* mice for 6 wk equipotently lowered plasma TG level (Vehi: 204 ± 18 mg/dl; bezafibrate: 95 ± 7, P < 0.01 mg/dl; fenofibrate: 85 ± 5 mg/dl, P < 0.01 vs. vehicle-treated *db/db* mice). Notably, treatment of bezafibrate (300 mg·kg^{-1}·day^{-1}) significantly lowered plasma glucose level at 6 wk with an equipotency to rosiglitazone (Vehi: 473 ± 24 mg/dl; bezafibrate: 216 ± 40 mg/dl, P < 0.01; fenofibrate: 408 ± 30 mg/dl, P = 0.10; rosiglitazone: 197 ± 23 mg/dl, P < 0.01 vs. vehicle-treated *db/db* mice). In the present study, we evaluated antidiabetic properties of bezafibrate and fenofibrate with the dose showing equipotent TG-lowering profile. In this context, TG-lowering profile in bezafibrate and fenofibrate in the present study indicates that the doses of drugs used were appropriate for assessing antidiabetic effects. Because we focused our special attention on PPARγ agonistic properties of bezafibrate, fenofibrate was employed as a "selective" PPARα agonist. Therefore, we evaluated two doses (100 or 300 mg·kg^{-1}·day^{-1}) of bezafibrate and a single dose (300 mg·kg^{-1}·day^{-1}) of fenofibrate.

Our results raise a couple of possibilities responsible for metabolically beneficial effects of bezafibrate. Decline of adiponectin levels is known (17, 33, 50) to associate with insulin resistance, hepatic fibrosis, and atherosclerosis in humans and rodents. In accordance with previous reports (10), plasma levels of adiponectin in *db/db* mice were significantly lower than those in vehicle-treated lean littermates (Fig. 1). Notably, bezafibrate significantly increased plasma adiponectin levels in *db/db* mice, whereas fenofibrate did not provoke such effects. More importantly, we demonstrated for the first time that bezafibrate pronouncedly augmented the expression and secretion of adiponectin in 3T3-L1 differentiated adipocytes (Fig. 5). Activation of PPARγ is known to increase plasma adiponectin levels in humans and rodents (27, 52). First, the present study confirmed that pioglitazone and rosiglitazone increased plasma adiponectin levels in *db/db* mice (Fig. 1*D*),

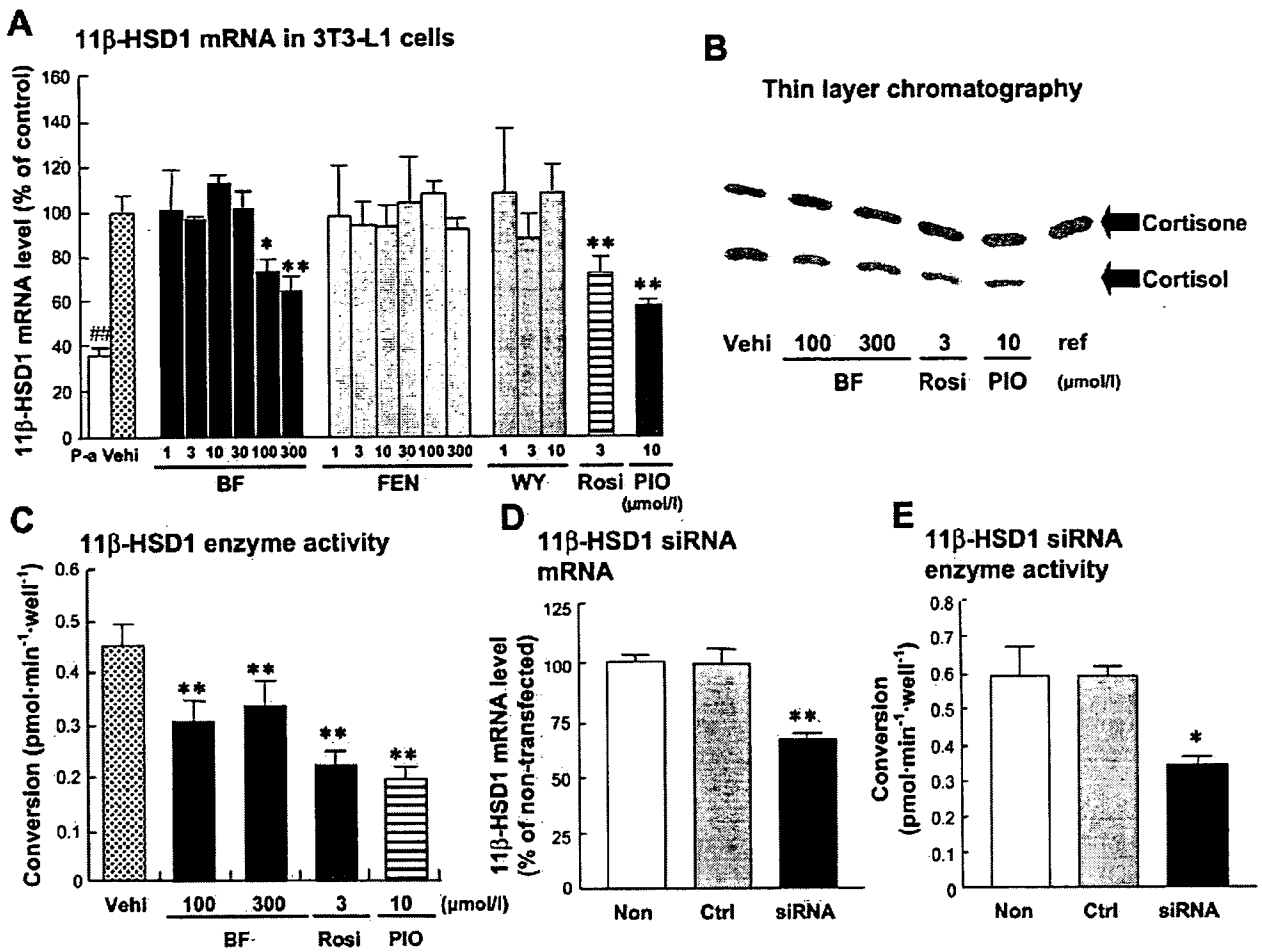

Fig. 4. 11 β-HSD1 mRNA levels (*A* and *D*) and oxoreductase activity (*B*, *C*, and *E*) in 3T3-L1 adipocytes. *A–C*: 3T3-L1 adipocytes were treated with BF (1–300 μmol/l), Rosi (3 μmol/l), PIO (10 μmol/l), FEN (1–300 μmol/l), WY-14,643 (WY; 1–10 μmol/l), or Vehi and 3T3-L1 preadipocytes (P-a) treated with vehicle for 48 h. *A*: each column represents %11β-HSD1 mRNA levels compared with vehicle-treated 3T3-L1 differentiated adipocytes (defined as 100%; $n = 6$). *B*: representative autoradiograph image of TLC; ref, cell-free control. *C*: each column shows 11β-HSD1 oxoreductase activity ($n = 3$). Data are presented as means ± SE. $^*P < 0.05$; $^{**}P < 0.01$ vs. vehicle-treated 3T3-L1 differentiated adipocytes; $^{\#\#}P < 0.01$ vs. vehicle-treated 3T3-L1 differentiated adipocytes. *D* and *E*: 3T3-L1 differentiated adipocytes were transfected with reagent only [nontrasfected control (Non)], nonsilencing control small interfering (si)RNA (Ctrl), or siRNA duplex-targeted 11β-HSD1 mRNA sequence. *D*: each column represents %11β-HSD1 mRNA levels compared with Non (defined as 100%; $n = 3$). *E*: each column shows 11β-HSD1 oxoreductase activity ($n = 3$). Data are presented as means ± SE. $^*P < 0.05$; $^{**}P < 0.01$ vs. nontransfected control.

and rosiglitazone induced adiponectin expression and secretion in 3T3-L1 differentiated adipocytes (Fig. 5). To date, there has been only one report (31) that bezafibrate significantly increased plasma adiponectin levels in obese-diabetic Otsuka Long-Evans Tokushima Fatty (OLETF) rats. Moreover, there were some reports (20, 21) showing that fenofibrate increased circulating adiponectin levels in humans. On the other hand, there was only one report (6) that fenofibrate increased mRNA levels of adiponectin in fat depots but did not increase serum levels in OLETF rats. A recent report (44) showed that WY-14,643, a selective PPARα agonist, did not increase serum adiponectin levels in obese-diabetic KKA^y mice. Collectively, the mechanistic link between PPARα activation and elevation of circulating adiponectin still remains unclear. In the present study, fenofibrate and WY-14,643 did not change adiponectin secretion in 3T3-L1 adipocytes, suggesting that PPARα activation by fenofibrate and WY-14,643 does not exert direct effects on adiponectin secretion. On the other hand, our data support the notion that bezafibrate directly influences adiponectin secretion in 3T3-L1 adipocytes. In contrast, several previous works (20, 21) have suggested that fenofibrate indirectly increased circulating adiponectin, presumably as a reflection of systemic improvement of fuel homeostasis. Our data suggest that bezafibrate-induced increase in plasma adiponectin levels is independent of PPARα activation. Thus, it is likely that a significant increase in adiponectin level induced by bezafibrate may be attributable to its PPARγ agonistic activity (48) and thus contribute, at least partly, to the improvement of glucose metabolism in *db/db* mice. Future investigations to see whether bezafibrate could increase circulating adiponectin level in humans will be of great interest.

A previous report (19) demonstrated that fenofibrate significantly reduced plasma leptin levels in OLETF rats. In the present study, bezafibrate and fenofibrate did not significantly change plasma leptin levels. In contrast, consistent with previous reports (34, 37, 51), pioglitazone decreased plasma leptin

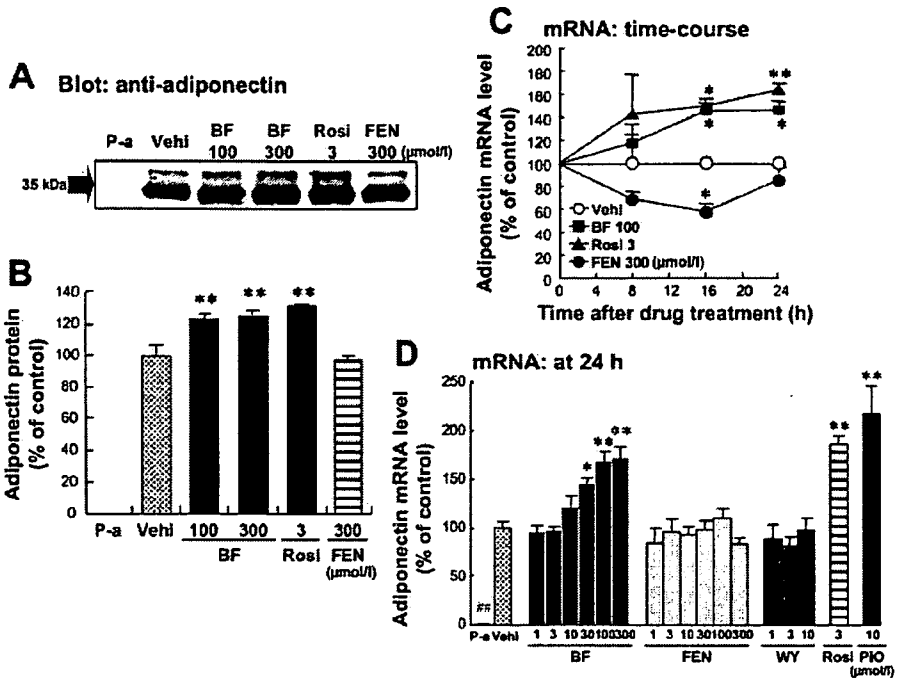

Fig. 5. Adiponectin protein and mRNA levels in 3T3-L1 preadipocytes (P-a) or differentiated adipocytes. *A*: representative Western blot. *B*: each column represents %adiponectin protein in cultured media quantified from Western blot compared with vehicle-treated 3T3-L1 differentiated adipocytes (defined as 100%; $n = 3$). *C* and *D*: adiponectin mRNA levels in 3T3-L1 adipocytes. Time course of adiponectin mRNA levels (*C*) in 3T3-L1 adipocytes treated with BF (100 μmol/l; ■), Rosi (3 μmol/l; ▲), FEN (300 μmol/l; ●), or Vehi (○) ($n = 3$) and adiponectin mRNA levels at 24 h ($n = 6$) (*D*). Data are presented as means + SE or means ± SE. $^*P < 0.05$; $^{**}P < 0.01$ vs. vehicle-treated 3T3-L1 differentiated adipocytes; $\#\#P < 0.01$ vs. vehicle-treated 3T3-L1 differentiated adipocytes.

levels, presumably via PPARγ activation in adipocytes (Fig. 1*C*). Taken together, a possible mechanistic link between PPARα activation and leptin regulation remains obscure. There were a couple of studies (6, 19) showing that fenofibrate decreased body weight, as well as adipose tissue weight, in OLETF rats. In the present study, both bezafibrate and fenofibrate treatments tended to increase body weight and mesenteric fat weight (Table 2). Because body weight increase was almost parallel to the increment in liver weight (Table 2), it is likely that weight gain in both groups was largely attributable to liver hypertrophy caused by PPARα activation.

Notably, with an equipotency to pioglitazone, bezafibrate markedly lowered the expression level of 11β-HSD1 in mesenteric fat (Fig. 3*B*). With a sharp contrast, fenofibrate did not change the expression of 11β-HSD1. Importantly, bezafibrate markedly lowered the expression and enzyme activity of 11β-HSD1 in 3T3-L1 differentiated adipocytes, equipotent to rosiglitazone and pioglitazone (Fig. 4). To our knowledge, this is the first demonstration that bezafibrate potently reduces mRNA expression and enzyme activity of 11β-HSD1 in cultured adipocytes. Our data clearly demonstrated that a knockdown of 11β-HSD1 by transfection of siRNA duplex significantly reduced mRNA expression and enzyme activity of 11β-HSD1 in 3T3-L1 differentiated adipocytes (Fig. 4, *D* and *E*), confirming that 11β-HSD1 acts as a distinct oxoreductase and activates glucocorticoid from inactive form. This result also validates the enzyme activity assays in the present study. It has been reported (4) that PPARγ agonists suppressed the expression levels of 11β-HSD1 mRNA exclusively in adipocytes. In accordance with this notion, in the present study, pioglitazone markedly suppressed the 11β-HSD1 mRNA in mesenteric and subcutaneous fat depots. Taken together, it is reasonable to speculate that bezafibrate suppresses 11β-HSD1 in fat depots via its agonistic property for PPARγ, thereby contributing, at least partly, to metabolically beneficial effects by bezafibrate.

It is important to note that the treatment of bezafibrate did not change circulating corticosterone levels in *db/db* mice in the present study. This indicates that, via the regulation of 11β-HSD1, bezafibrate modifies intracellular glucocorticoid metabolism in a tissue- or cell-specific manner but does not affect systemic glucocorticoid homeostasis. The present study demonstrated that bezafibrate, fenofibrate, and pioglitazone significantly decreased 11β-HSD1 mRNA levels in liver (Fig. 3*A*). These effects may also explain unidentified, metabolically beneficial properties of fibrates (13, 25), because transgenic mice overexpressing 11β-HSD1 exclusively in liver exemplify fatty liver, glucose intolerance, dyslipidemia, and severe hypertension (36). In this context, the potential pathophysiological role of 11β-HSD1 in liver must await further investigation.

Bezafibrate has been characterized as a PPAR(α, -γ, and -δ) pan-agonist in vitro (9, 48). It was reported (24, 40, 42) that GW501516, known as a PPARδ agonist, exerts beneficial effects on insulin resistance. Thus, the activation of PPARδ by bezafibrate may also contribute to its metabolically beneficial effects. Although physiological relevance and an entire picture of the mechanism whereby bezafibrate ameliorates fuel dyshomeostasis in humans must await further investigation, our results presented here provide novel evidence that bezafibrate directly regulates 11β-HSD1 and adiponectin in murine adipocytes. Further investigations on other rodent models and human clinics should validate its accuracy and may open a fresh avenue for therapeutic strategies that might target convergence of multiple risk factors.

GRANTS

This work was supported in part by a Grant-in-Aid for Scientific Research (B2, 16390267), a Grant-in-Aid for Scientific Research on Priority Areas (Adipomics, 15081101), a Grant-in-Aid for Research on Measures for Intractable Diseases (Health and Labor Science Research Grant), a Research Grant from Special Coordination Funds for Promoting Science and Technology, and

grants from the National Cardiovascular Center, Smoking Research Foundation, Metabolic Syndrome Foundation, and Setsuro Fujii Memorial Osaka Foundation.

REFERENCES

1. **Alberts P, Engblom L, Edling N, Forsgren M, Klingstrom G, Larsson C, Ronquist-Nii Y, Ohman B, Abrahmsen L.** Selective inhibition of 11beta-hydroxysteroid dehydrogenase type 1 decreases blood glucose concentrations in hyperglycaemic mice. *Diabetologia* 45: 1528–1532, 2002.
2. **Asayama K, Sandhir R, Sheikh FG, Hayashibe H, Nakane T, Singh I.** Increased peroxisomal fatty acid beta-oxidation and enhanced expression of peroxisome proliferator-activated receptor-alpha in diabetic rat liver. *Mol Cell Biochem* 194: 227–234, 1999.
3. **Bays H, Stein EA.** Pharmacotherapy for dyslipidaemia—current therapies and future agents. *Expert Opin Pharmacother* 4: 1901–1938, 2003.
4. **Berthiaume M, Sell H, Lalonde J, Gelinas Y, Tchernof A, Richard D, Deshaies Y.** Actions of PPARγ agonism on adipose tissue remodeling, insulin sensitivity, and lipemia in absence of glucocorticoids. *Am J Physiol Regul Integr Comp Physiol* 287: R1116–R1123, 2004.
5. **Bujalska IJ, Kumar S, Stewart PM.** Dose central obesity reflect "Cushing's disease of the omentum"? *Lancet* 349: 1210–1213, 1997.
6. **Choi KC, Ryu OH, Lee KW, Kim HY, Seo JA, Kim SG, Kim NH, Choi DS, Baik SH, Choi KM.** Effect of PPAR-alpha and -gamma agonist on the expression of visfatin, adiponectin, and TNF-alpha in visceral fat of OLETF rats. *Biochem Biophys Res Commun* 336: 747–53, 2005.
7. **Folch J, Lees M, Sloane Stanley GH.** A simple method for the isolation and purification of total lipids from animal tissues. *J Biol Chem* 226: 497–509, 1957.
8. **Frost SC, Lane MD.** Effect of phenylarsine oxide on insulin-dependent protein phosphorylation and glucose transport in 3T3-L1 adipocytes. *J Biol Chem* 262: 9872–9876, 1985.
9. **Fruchart JC, Staels B, Duriez P.** The role of fibric acids in atherosclerosis. *Curr Atheroscler Rep* 3: 83–92, 2001.
10. **Fujita H, Fujishima H, Koshimura J, Hosoba M, Yoshioka N, Shimotomai T, Morii T, Narita T, Kakei M, Ito S.** Effects of antidiabetic treatment with metformin and insulin on serum and adipose tissue adiponectin levels in db/db mice. *Endocr J* 52: 427–433, 2005.
11. **Goa KL, Barradell LB, Plosker GL.** Bezafibrate. An update of its pharmacology and use in the management of dyslipidaemia. *Drugs* 52: 725–753, 1996.
12. **Haubenwallner S, Essenburg AD, Barnett BC, Pape ME, DeMattos RB, Krause BR, Minton LL, Auerbach BJ, Newton RS, Leff T, Bisgaierl CL.** Hypolipidemic activity of select fibrates correlates to changes in hepatic apolipoprotein C-III expression: a potential physiologic basis for their mode of action. *J Lipid Res* 36: 2541–2551, 1995.
13. **Hermanowski-Vosatka A, Gerholdb D, Mundta SS, Lovinga VA, Lub M, Chenc Y, Elbrechtc A, Wuc M, Doebberc T, Kellyc L, Milota D, Guoa Q, Wanga PR, Ippolitoa M, Chaoa YS, Wrighta SD, Thieringer R.** PPARα agonists reduce 11β-hydroxysteroid dehydrogenase type 1 in the liver. *Biochem Biophys Res Commun* 279: 330–336, 2000.
14. **Hrebicek J.** PPARs: the role in glucose and lipid homeostasis, insulin resistance and atherosclerosis. *Cesk Fysiol* 53: 4–16, 2004.
15. **Jones IR, Swai A, Taylor R, Miller M, Laker MF, Alberti KG.** Lowering of plasma glucose concentrations with bezafibrate in patients with moderately controlled NIDDM. *Diabetes Care* 13: 855–863, 1990.
16. **Joseph JW, Koshkin V, Zhang CY, Wang J, Lowell BB, Chan CB, Wheeler MB.** Uncoupling protein 2 knockout mice have enhanced insulin secretory capacity after a high-fat diet. *Diabetes* 51: 3211–3219, 2002.
17. **Kamada Y, Tamura S, Kiso S, Matsumoto H, Saji Y, Yoshida Y, Fukui K, Maeda N, Nishizawa H, Nagaretani H, Okamoto Y, Kihara S, Miyagawa J, Shinomura Y, Funahashi T, Matsuzawa Y.** Enhanced carbon tetrachloride-induced liver fibrosis in mice lacking adiponectin. *Gastroenterology* 125: 1796–1807, 2003.
18. **Kershaw EE, Morton NM, Dhillon H, Ramage L, Seckl JR, Flier JS.** Adipocyte-specific glucocorticoid inactivation protects against diet-induced obesity. *Diabetes* 54: 1023–1031, 2005.
19. **Koh EH, Kim MS, Park JY, Kim HS, Youn JY, Park HS, Youn JH, Lee KU.** Peroxisome proliferator-activated receptor (PPAR)-alpha activation prevents diabetes in OLETF rats: comparison with PPAR-gamma activation. *Diabetes* 52: 2331–2337, 2003.
20. **Koh KK, Han SH, Quon MJ, Yeal Ahn J, Shin EK.** Beneficial effects of fenofibrate to improve endothelial dysfunction and raise adiponectin levels in patients with primary hypertriglyceridemia. *Diabetes Care* 28: 1419–1424, 2005.
21. **Koh KK, Quon MJ, Han SH, Chung WJ, Ahn JY, Seo YH, Choi IS, Shin EK.** Additive beneficial effects of fenofibrate combined with atorvastatin in the treatment of combined hyperlipidemia. *J Am Coll Cardiol* 45: 1649–1653, 2005.
22. **Kuwabara K, Murakami K, Todo M, Aoki T, Asaki T, Murai M, Yano J.** A novel selective peroxisome proliferator-activated receptor alpha agonist, 2-methyl-c-5[4-[5-methyl-2-(4-methylphenyl)-4-oxazolyl]butyl]-1,3-dioxane-r-2-carboxylic acid (NS-220), potently decreases plasma triglyceride and glucose levels and modifies lipoprotein profiles in KK-Ay mice. *J Pharmacol Exp Ther* 309: 970–977, 2004.
23. **Laemmli UK.** Cleavage of structural proteins during the assembly of the head of bacteriophage T4. *Nature* 227: 680–685, 1970.
24. **Lee CH, Olson P, Hevener A, Mehl I, Chong LW, Olefsky JM, Gonzalez FJ, Ham J, Kang H, Peters JM, Evans RM.** PPARdelta regulates glucose metabolism and insulin sensitivity. *Proc Natl Acad Sci USA* 103: 3444–3449, 2006.
25. **Lee HJ, Choi SS, Park MK, An YJ, Seo SY, Kim MC, Hong SH, Hwang TH, Kang DY, Garber AJ, Kim DK.** Fenofibrate lowers abdominal and skeletal adiposity and improves insulin sensitivity in OLETF rats. *Biochem Biophys Res Commun* 296: 293–299, 2002.
26. **Maeda N, Shimomura I, Kishida K, Nishizawa H, Matsuda M, Nagaretani H, Furuyama N, Kondo H, Takahashi M, Arita Y, Komuro R, Ouchi N, Kihara S, Tochino Y, Okutomi K, Horie M, Takeda S, Aoyama T, Funahashi T, Matsuzawa Y.** Diet-induced insulin resistance in mice lacking adiponectin/ACRP30. *Nat Med* 8: 731–737, 2002.
27. **Maeda N, Takahashi M, Funahashi T, Kihara S, Nishizawa H, Kishida K, Nagaretani H, Matsuda M, Komuro R, Ouchi N, Kuriyama H, Hotta K, Nakamura T, Shimomura I, Matsuzawa Y.** PPARγ ligands increase expression and plasma concentrations of adiponectin, an adipose-derived protein. *Diabetes* 50: 2094–2099, 2001.
28. **Masuzaki H, Flier JS.** Tissue-specific glucocorticoid reactivating enzyme, 11 beta-hydroxysteroid dehydrogenase type 1 (11 beta-HSD1)—a promising drug target for the treatment of metabolic syndrome. *Curr Drug Targets Immune Endocr Metabol Disord* 3: 255–262, 2003.
29. **Masuzaki H, Paterson J, Shinyama H, Morton NM, Mullins JJ, Seckl JR, Flier JS.** A transgenic model of visceral obesity and the metabolic syndrome. *Science* 294: 2166–2170, 2001.
30. **Masuzaki H, Yamamoto H, Kenyon CJ, Elmquist JK, Morton NM, Paterson JM, Shinyama H, Sharp MG, Fleming S, Mullins JJ, Seckl JR, Flier JS.** Transgenic amplification of glucocorticoid action in adipose tissue causes high blood pressure in mice. *J Clin Invest* 112: 83–90, 2003.
31. **Mori Y, Oana F, Matsuzawa A, Akahane S, Tajima N.** Short-term effect of bezafibrate on the expression of adiponectin mRNA in the adipose tissues. *Endocrine* 25: 247–251, 2004.
32. **Morton NM, Paterson JM, Masuzaki H, Holmes MC, Staels B, Fievet C, Walker BR, Flier JS, Mullins JJ, Seckl JR.** Novel adipose tissue-mediated resistance to diet-induced visceral obesity in 11β-hydroxysteroid dehydrogenase type 1-deficient mice. *Diabetes* 53: 931–938, 2004.
33. **Okamoto Y, Kihara S, Ouchi N, Nishida M, Arita Y, Kumada M, Ohashi K, Sakai N, Shimomura I, Kobayashi H, Terasaka N, Inaba T, Funahashi T, Matsuzawa Y.** Adiponectin reduces atherosclerosis in apolipoprotein E-deficient mice. *Circulation* 106: 2767–2770, 2002.
34. **Pickavance LC, Tadayyon M, Widdowson PS, Buckingham RE, Wilding JP.** Therapeutic index for rosiglitazone in dietary obese rats: separation of efficacy and haemodilution. *Br J Pharmacol* 128: 1570–1576, 1999.
35. **Purves RD.** Optimum numerical integration methods for estimation of area-under-the-curve (AUC) and area-under-the-moment-curve (AUMC). *J Pharmacokinet Biopharm* 20: 211–226, 1992.
36. **Paterson JM, Morton NM, Fievet C, Kenyon CJ, Holmes MC, Staels B, Seckl JR, Mullins JJ.** Metabolic syndrome without obesity: hepatic overexpression of 11beta-hydroxysteroid dehydrogenase type 1 in transgenic mice. *Proc Natl Acad Sci USA* 101: 7088–7093, 2004.
37. **Rasouli N, Yao-Borengasser A, Miles LM, Elbein SC, Kern PA.** Increased plasma adiponectin in response to pioglitazone does not result from increased gene expression. *Am J Physiol Endocrinol Metab* 290: E42–E46, 2006.
38. **Seckl JR, Walker BR.** Minireview: 11beta-hydroxysteroid dehydrogenase type 1—a tissue-specific amplifier of glucocorticoid action. *Endocrinology* 142: 1371–1376, 2001.
39. **Sleeman MW, Garcia K, Liu R, Murray JD, Malinova L, Moncrieffe M, Yancopoulos GD, Wiegand SJ.** Ciliary neurotrophic factor improves

diabetic parameters and hepatic steatosis and increases basal metabolic rate in db/db mice. *Proc Natl Acad Sci USA* 100: 14297–14302, 2003.

40. **Takahashi S, Tanaka T, Kodama T, Sakai J.** Peroxisome proliferator-activated receptor delta (PPARdelta), a novel target site for drug discovery in metabolic syndrome. *Pharmacol Res* 53: 501–507, 2006.
41. **Tanaka T, Masuzaki H, Ebihara K, Ogawa Y, Yasue S, Yukioka H, Chusho H, Miyanaga F, Miyazawa T, Fujimoto M, Kusakabe T, Kobayashi N, Hayashi T, Hosoda K, Nakao K.** Transgenic expression of mutant peroxisome proliferator-activated receptor (PPAR)γ in liver precipitates fasting-induced steatosis but protects against high fat diet-induced steatosis in mice. *Metabolism* 54: 1490–1498, 2005.
42. **Tanaka T, Yamamoto J, Iwasaki S, Asaba H, Hamura H, Ikeda Y, Watanabe M, Magoori K, Ioka RX, Tachibana K, Watanabe Y, Uchiyama Y, Sumi K, Iguchi H, Ito S, Doi T, Hamakubo T, Naito M, Auwerx J, Yanagisawa M, Kodama T, Sakai J.** Activation of peroxisome proliferator-activated receptor delta induces fatty acid beta-oxidation in skeletal muscle and attenuates metabolic syndrome. *Proc Natl Acad Sci USA* 100: 15924–15929, 2003.
43. **Tenenbaum A, Motro M, Fisman EZ, Schwammenthal E, Adler Y, Goldenberg I, Leor J, Boyko V, Mandelzweig L, Behar S.** Peroxisome proliferator-activated receptor ligand bezafibrate for prevention of type 2 diabetes mellitus in patients with coronary artery disease. *Circulation* 109: 2197–2202, 2004.
44. **Tsuchida A, Yamauchi T, Takekawa S, Hada Y, Ito Y, Maki T, Kadowaki T.** Peroxisome proliferator-activated receptor PPARalpha activation increases adiponectin receptors and reduces obesity-related inflammation in adipose tissue: comparison of activation of PPARalpha, PPARgamma, and their combination. *Diabetes* 54: 3358–3370, 2005.
45. **Vanden Heuvel JP.** Peroxisome proliferator-activated receptors (PPARs) and carcinogenesis. *Toxicol Sci* 47: 1–8, 1999.
46. **Verges B.** Clinical interest of PPARs ligands. *Diabetes Metab* 30: 7–12, 2004.
47. **Whorwood CB, Donovan SJ, Flanagan D, Phillips DI, Byrne CD.** Increased glucocorticoid receptor expression in human skeletal muscle cells may contribute to the pathogenesis of the metabolic syndrome. *Diabetes* 51: 1066–1075, 2002.
48. **Willson TM, Brown PJ, Sternbach DD, Henke BR.** The PPARs: from orphan receptors to drug discovery. *J Med Chem* 43: 527–550, 2000.
49. **Wolfrum C, Ellinghaus P, Fobker M, Seedorf U, Assmann G, Borchers T, Spener F.** Phytanic acid is ligand and transcriptional activator of murine liver fatty acid binding protein. *J Lipid Res* 40: 708–714, 1999.
50. **Yamauchi T, Kamon J, Waki H, Terauchi Y, Kubota N, Hara K, Mori Y, Ide T, Murakami K, Tsuboyama-Kasaoka N, Ezaki O, Akanuma Y, Gavrilova O, Vinson C, Reitman ML, Kagechika H, Shudo K, Yoda M, Nakano Y, Tobe K, Nagai R, Kimura S, Tomita M, Froguel P, Kadowaki T.** The fat-derived hormone adiponectin reverses insulin resistance associated with both lipoatrophy and obesity. *Nat Med* 7: 941–946, 2001.
51. **Ye JM, Doyle PJ, Iglesias MA, Watson DG, Cooney GJ, Kraegen EW.** Peroxisome proliferator-activated receptor (PPAR)-alpha activation lowers muscle lipids and improves insulin sensitivity in high fat-fed rats: comparison with PPAR-gamma activation. *Diabetes* 50: 411–417, 2001.
52. **Yilmaz MI, Sonmez A, Caglar K, Gok DE, Eyileten T, Yenicesu M, Acikel C, Bingol N, Kilic S, Oguz Y, Vural A.** Peroxisome proliferator-activated receptor gamma (PPAR-gamma) agonist increases plasma adiponectin levels in type 2 diabetic patients with proteinuria. *Endocrine* 25: 207–214, 2004.

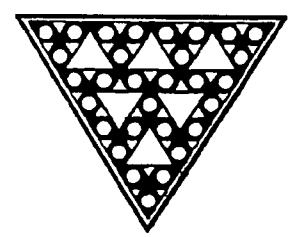

J Appl Physiol 102: 1007–1013, 2007.
First published November 22, 2006; doi:10.1152/japplphysiol.01034.2006.

Effect of acute activation of 5′-AMP-activated protein kinase on glycogen regulation in isolated rat skeletal muscle

Licht Miyamoto,[1] Taro Toyoda,[2] Tatsuya Hayashi,[1,3] Shin Yonemitsu,[1] Masako Nakano,[1] Satsuki Tanaka,[1] Ken Ebihara,[1] Hiroaki Masuzaki,[1] Kiminori Hosoda,[1] Yoshihiro Ogawa,[1] Gen Inoue,[1] Tohru Fushiki,[2] and Kazuwa Nakao[1]

[1]*Department of Medicine and Clinical Science, Graduate School of Medicine,* [2]*Laboratory of Nutrition Chemistry, Division of Food Science and Biotechnology, Graduate School of Agriculture, and* [3]*Laboratory of Sports and Exercise Medicine, Graduate School of Human and Environmental Studies, Kyoto University, Kyoto, Japan*

Submitted 15 September 2006; accepted in final form 19 November 2006

Miyamoto L, Toyoda T, Hayashi T, Yonemitsu S, Nakano M, Tanaka S, Ebihara K, Masuzaki H, Hosoda K, Ogawa Y, Inoue G, Fushiki T, Nakao K. Effect of acute activation of 5′-AMP-activated protein kinase on glycogen regulation in isolated rat skeletal muscle. *J Appl Physiol* 102: 1007–1013, 2007. First published November 22, 2006; doi:10.1152/japplphysiol.01034.2006.—5′-AMP-activated protein kinase (AMPK) has been implicated in glycogen metabolism in skeletal muscle. However, the physiological relevance of increased AMPK activity during exercise has not been fully clarified. This study was performed to determine the direct effects of acute AMPK activation on muscle glycogen regulation. For this purpose, we used an isolated rat muscle preparation and pharmacologically activated AMPK with 5-aminoimidazole-4-carboxamide-1-β-D-ribonucleoside (AICAR). Tetanic contraction in vitro markedly activated the α_1- and α_2-isoforms of AMPK, with a corresponding increase in the rate of 3-*O*-methylglucose uptake. Incubation with AICAR elicited similar enhancement of AMPK activity and 3-*O*-methylglucose uptake in rat epitrochlearis muscle. In contrast, whereas contraction stimulated glycogen synthase (GS), AICAR treatment decreased GS activity. Insulin-stimulated GS activity also decreased after AICAR treatment. Whereas contraction activated glycogen phosphorylase (GP), AICAR did not alter GP activity. The muscle glycogen content decreased in response to contraction but was unchanged by AICAR. Lactate release was markedly increased when muscles were stimulated with AICAR in buffer containing glucose, indicating that the glucose taken up into the muscle was catabolized via glycolysis. Our results suggest that AMPK does not mediate contraction-stimulated glycogen synthesis or glycogenolysis in skeletal muscle and also that acute AMPK activation leads to an increased glycolytic flux by antagonizing contraction-stimulated glycogen synthesis.

contraction; glycogen synthase; glycogen phosphorylase; epitrochlearis muscle; glycolysis

EXERCISE PROFOUNDLY AFFECTS glycogen metabolism by stimulating glycogenolysis during exercise, which is followed by the resynthesis of glycogen after exercise. Intracellular glycogen plays a major role as a fuel for acute muscle contraction, and its concentration is dramatically reduced in response to a single bout of exercise (6, 14, 25, 38). The facilitation of glycogen resynthesis after exercise causes a marked accumulation of glycogen, i.e., the well-known phenomenon of glycogen supercompensation. Similar to exercise, insulin causes strong glucose uptake and glycogen synthesis. Therefore, the increase in insulin sensitivity in skeletal muscle after exercise also plays an important role in glucose metabolism (11, 25, 36). In contrast to the physiological relevance of muscle glycogen, the signaling mechanisms leading to the regulation of glycogen synthesis and glycogenolysis in contracting muscle have not been fully clarified.

Several aspects of the contraction-evoked metabolic events in skeletal muscle have been shown to be related to 5′-AMP-activated protein kinase (AMPK), including GLUT4 translocation and glucose transport (1, 4, 18, 19, 27, 31, 32), fatty acid oxidation via the inactivation of acetyl-CoA carboxylase (23, 32, 41, 43), GLUT4 expression (7, 21, 22, 32, 35, 44, 48), and insulin sensitivity (12, 24, 32). AMPK, a heterotrimeric serine/threonine protein kinase, consists of a catalytic α-subunit and regulatory β- and γ-subunits. Two distinct α-isoforms, α_1 and α_2, are expressed in skeletal muscle (39), and both isoforms can be activated in response to muscle contraction (40). AMPK is allosterically activated in response to an elevation in AMP concentration or in the AMP-to-ATP ratio. It is also activated when phosphorylated by upstream kinases (42, 46). Therefore, it has been hypothesized that AMPK acts as an intracellular energy sensor that plays a key role in regulating cellular metabolism in skeletal muscle (9, 13, 18, 19, 23, 37, 41, 43).

Recent studies of natural and manipulated mutations in AMPK suggest that chronic changes in AMPK action have substantial effects on glycogen metabolism in skeletal muscle. The glycogen concentration in the gastrocnemius muscles of mice that muscle-specifically express a dominant-negative kinase-dead form of the α-isoform is about half that observed in nontransgenic mice (31), although glycogen synthase (GS) activity and glycogen phosphorylase (GP) activity are not significantly different between the transgenic and nontransgenic animals under basal conditions or after contraction (30). The AMPK R225Q mutation in the *PRKAG3* gene, which encodes the muscle-specific isoform of the γ_3-subunit of AMPK, leads to increased glycogen accumulation in Hampshire pig skeletal muscle (29). The amount of glycogen in the gastrocnemius muscle is twofold higher in the R225Q *PRKAG3* transgenic mouse than in the wild-type mouse but is unaltered in the *PRKAG3*-null mouse (5). In contrast, another mutation has been identified in the pig *PRKAG3* gene (V224I) that is associated with low muscle glycogen (10). It has also been suggested that mutations in *PRKAG2*, the gene for the γ_2-subunit of AMPK, cause glycogen-associated vacuoles to

Address for reprint requests and other correspondence: T. Hayashi, Laboratory of Sports and Exercise Medicine, Graduate School of Human and Environmental Studies, Kyoto Univ., Yoshida-nihonmatsu-cho, Sakyo-ku, Kyoto 606-8501, Japan (e-mail: tatsuya@kuhp.kyoto-u.ac.jp).

The costs of publication of this article were defrayed in part by the payment of page charges. The article must therefore be hereby marked "*advertisement*" in accordance with 18 U.S.C. Section 1734 solely to indicate this fact.

form in myocytes, leading to a glycogen storage disease of the cardiac muscle (2).

The physiological relevance of the acute elevation of AMPK activity during exercise to muscle glycogen regulation has not been fully elucidated. Halse et al. (16) reported GS inactivation in accordance with AMPK activation after 2 h of glucose starvation in the medium in human myoblast cells in culture. They also showed that stimulation by 5-aminoimidazole-4-carboxamide-1-β-D-ribonucleoside (AICAR) or hydrogen peroxide caused AMPK activation and concurrent GS inactivation. Wojtaszewski et al. (45) demonstrated that the addition of AICAR to the circulation medium resulted in increased AMPK-α_2 activity and decreased GS activity in perfused rat skeletal muscles. AICAR is taken up into muscle cells and metabolized to form ZMP, a monophosphorylated derivative that mimics the stimulatory effects of AMP on AMPK without changing the concentration of AMP or ATP (17). In fact, GS Ser^7 can be phosphorylated and inactivated by AMPK in vitro (8) and in vivo (26). Wojtaszewski et al. also found significant activation of α_2-AMPK and inactivation of GS when muscle glycogen was depleted by prolonged exercise and restricted diet. In contrast, repeated activation of AMPK by the administration of AICAR for 5–28 days increased glycogen concentration in rat skeletal muscles (7, 21, 44). Aschenbach et al. (3) demonstrated acute activation of AMPK-α_2 in red and white gastrocnemius muscles in normal rats after a single intraperitoneal dose of AICAR. However, GS activity was reduced only in white gastrocnemius muscle, whereas GS activity conversely increased in red gastrocnemius muscle (3). They also made the contradictory observation that in vitro incubation with AICAR had no effect on GS activity in isolated rat muscles (epitrochlearis or flexor digitorum brevis) (3).

Therefore, we undertook the present study to elucidate the direct effects of acute AMPK activation, which is comparable to activation in contracting muscle on glycogenolysis and glycogen synthesis in mature skeletal muscle. For this purpose, we used an isolated rat muscle preparation and pharmacologically manipulated muscle AMPK with AICAR stimulation, which allowed us to activate AMPK-α_1 and -α_2 to a level similar to that observed after tetanic contraction in skeletal muscle. We demonstrate that activation of AMPK, in contrast to muscle contraction, does not cause GS or GP activation, nor does it cause a decrease in muscle glycogen. We propose that AMPK activation per se antagonizes glycogen synthesis in contracting muscle and facilitates the regeneration of ATP via glycolysis.

MATERIALS AND METHODS

Materials. All radioactive materials ([γ-^{32}P]ATP, 3-*O*-methyl-[^{3}H]glucose, [^{14}C]mannitol, [^{14}C]UDP-glucose, and [^{14}C]glucose 1-phosphate) were obtained from Perkin Elmer Japan (Yokohama, Japan), human insulin (Humulin R) from Eli Lilly (Indianapolis, IN), P81 filter paper from Whatman (Brentford, UK), and protein A-Sepharose from GE Healthcare Bioscience (Little Chalfont, UK). All other reagents were of analytic grade and were obtained from Sigma-Aldrich (St. Louis, MO), unless otherwise stated.

Animals. Male Sprague-Dawley rats (120–130 g body wt; Japan SLC, Hamamatsu, Japan) were housed in an animal facility maintained at 20°C with a 12:12-h light-dark cycle and allowed free access to water and standard rodent chow. After an overnight fast, the rats were randomly assigned to experimental groups. The Kyoto University Graduate School of Medicine Committee on Animal Research approved all experimental procedures.

Muscle sample preparation. Animals were killed by cervical dislocation. The epitrochlearis muscles were rapidly isolated and incubated as previously described (19), with some modifications. Briefly, the muscles were preincubated for 40 min in 6 ml of Krebs-Ringer bicarbonate (KRB) buffer, pH 7.4, containing 2 mM sodium pyruvate (KRB-P). For the dose-response and time-course changes in AICAR-stimulated AMPK activity, muscles were incubated in the absence or presence of AICAR (0.03, 0.125, 0.5, 2, or 8 mM) for 40 min or in the presence of 2 mM AICAR for 10, 30, 40, or 60 min, respectively. On the basis of these experiments, we decided to stimulate muscles with 2 mM AICAR for 40 min in other experiments (see RESULTS). For insulin treatment, muscles were preincubated and then incubated in the presence of 1 μM insulin for 40 min. For epinephrine treatment, muscles were preincubated and then incubated in the presence of 3 μg/ml epinephrine for the last 15 min of the incubation period (total 40 min). Muscle contractions were induced by preincubation of muscles and then incubation in KRB-P for 40 min, followed by electrical stimulation during the last 10 min, as described previously (19) (1/min train rate, 10-s train duration, 100-Hz pulse rate, 0.1-ms pulse duration, 100 V). The buffers were continuously gassed with 95% O_2-5% CO_2 and maintained at 37°C. The muscles were then used for glucose uptake measurements (see *Glucose uptake*) or trimmed and immediately frozen in liquid nitrogen for other assays. For the measurement of lactate release, we used KRB containing 8 mM glucose during preincubation and stimulation. AICAR treatment and muscle contractions were performed as described above.

Isoform-specific AMPK activity. AMPK activity was determined as described previously, with slight modifications (40). Frozen muscles were homogenized in ice-cold lysis buffer (1:60, wt/vol) containing 20 mM HEPES (pH 7.4), 1% Triton X-100, 50 mM sodium chloride, 50 mM sodium fluoride, 5 mM sodium pyrophosphate, 2 mM dithiothreitol, 4 mg/l leupeptin, 50 mg/l trypsin inhibitor, 0.1 mM benzamidine, and 0.5 mM phenylmethylsulfonyl fluoride and then centrifuged at 14,000 *g* for 20 min at 4°C. The supernatants (200 μg of protein) were immunoprecipitated with isoform-specific antibodies directed against the α_1- or α_2-subunit of AMPK (40) and protein A-Sepharose beads. The immune complex was washed extensively with 240 mM HEPES (pH 7.0) and 480 mM sodium chloride. Kinase activity was determined by the phosphorylation of the SAMS peptide (40). The kinase reaction was carried out in 40 mM HEPES (pH 7.0), 0.1 mM SAMS, 0.2 mM AMP, 80 mM sodium chloride, 0.8 mM dithiothreitol, 5 mM magnesium chloride, and 0.2 mM ATP (2 μCi of [γ-^{32}P]ATP) for 20 min at 30°C. The reaction products were then spotted onto P81 filter papers, which were extensively washed in 1% phosphoric acid, and the radioactivity on the dried papers was quantified with a liquid scintillation counter (Aloka, Tokyo, Japan).

Glucose uptake. We evaluated 3-*O*-methylglucose (3-MG) uptake as an index of glucose uptake activity. 3-MG uptake was determined as described previously (19), with modifications. After the incubation period, muscles were incubated in KRB containing 1 mM 3-MG, 1.5 μCi/ml [^{3}H]3-MG, 7 mM mannitol, and 0.3 μCi/ml [^{14}C]mannitol at 30°C for 10 min. The muscles were then trimmed and frozen in liquid nitrogen. The muscles were processed by incubation in 1 M NaOH at 85°C for 10 min, and the digestates were neutralized with HCl. The radioactivity in aliquots of the digestates was determined by liquid scintillation counting of dual labels, and the extracellular and intracellular spaces were calculated. The rate of 3-MG uptake was expressed as micromoles of 3-MG per milliliter of intracellular space per hour.

GS activity. GS activity was determined as described previously (19), with modifications. Frozen muscles were homogenized in lysis buffer (*buffer A*) containing 20 mM HEPES (pH 7.4), 1% Triton X-100, 50 mM sodium chloride, 50 mM sodium fluoride, 5 mM sodium pyrophosphate, 2 mM EGTA, 50 mM β-glycerophosphate, 4 mg/l leupeptin, 10 μg/ml aprotinin, 3 mM benzamidine, and 0.5 mM

phenylmethylsulfonyl fluoride and centrifuged at 14,000 *g* at 4°C for 30 min. The supernatants (40 μg of protein) were added to 80 μl of assay mixture containing 50 mM Tris (pH 7.8), 5 mM EDTA, 6.7 mM UDP-glucose, 10 mg/ml glycogen, 50 mM β-glycerophosphate, 50 mM sodium fluoride, and 0.1 mCi/mmol [^{14}C]UDP-glucose at 30°C, in the absence and presence of 10 mM glucose 6-phosphate (G-6-P), to measure G-6-P-independent (active form) and total GS activities, respectively. After 15 min the reaction solution was spotted onto a filter paper to terminate the reaction. The filter papers were washed extensively in 66% (vol/vol) ice-cold ethanol and then evaluated in a liquid scintillation counter for ^{14}C incorporation into glycogen. GS activity in the muscle was expressed as the active form ratio: G-6-P-independent activity ÷ total GS activity. The effect of ZMP on basal GS activity was evaluated by measurement of absolute GS activity in the presence of 6 mM ZMP, instead of 10 mM G-6-P, in the assay mixture. Absolute GS activity was expressed as ^{14}C incorporation activity (nmol·min^{-1}·mg protein^{-1}).

GP activity. Muscle GP activity was measured as described previously (15). Frozen muscles were homogenized in *buffer A*, and the supernatants were prepared as described for GS activity. Supernatants (40 μg of protein) were added to 80 μl of assay mixture containing 50 mM MES (pH 6.1), 100 mM glucose 1-phosphate, 200 mM potassium fluoride, 10 mg/ml glycogen, and 2.5 mCi/mol [^{14}C]glucose 1-phosphate, in the absence and presence of 6 mM 5′-AMP, to measure AMP-independent and total GP activities, respectively. After 15 min the reaction solution was spotted onto a filter paper to terminate the reaction. The papers were washed extensively in 66% (vol/vol) ice-cold ethanol and then evaluated in a liquid scintillation counter for ^{14}C incorporation into glycogen. GP activity in the muscle was expressed as the active form ratio: 5′-AMP-independent activity ÷ total GP activity. The effect of ZMP on basal GP activity was evaluated by measurement of absolute GP activity in the presence of 6 mM ZMP, instead of 6 mM 5′-AMP, in the assay mixture. Absolute GP activity was expressed as ^{14}C incorporation activity (μmol·min^{-1}·mg protein^{-1}).

Muscle glycogen. Frozen muscles were processed by incubation in 1 M NaOH at 85°C for 10 min. The digestates were neutralized with HCl. The glycogen in the digestates was hydrolyzed by incubation in 2 N HCl for 2 h at 85°C. The digestates were neutralized with NaOH, and the glucose released from the glycogen was measured enzymatically using a hexokinase glucose assay reagent (Sigma-Aldrich). Glycogen content was expressed as micromoles of glucosyl unit per gram wet muscle weight.

Lactate. Muscles were incubated and stimulated in KRB containing 8 mM glucose as described above. After muscle contraction for 10 min or AICAR stimulation for 40 min, aliquots of the incubation buffer were collected, and the lactate in the buffer was determined using the Determiner-LA kit (Kyowa Medex, Tokyo, Japan). The lactate released into the buffer was calculated and normalized to the wet muscle weight.

Statistical analysis. Values are means ± SE. Multiple means were compared by ANOVA. Two means were compared by Student's *t*-test. $P < 0.05$ was considered statistically significant.

RESULTS

AICAR acutely stimulates muscle AMPK in a dose- and time-dependent manner to a level comparable to that achieved by contraction. To evaluate the effects of AICAR stimulation on rat epitrochlearis muscle, we determined the dose and time dependency of its effects on isoform-specific AMPK activities. Pharmacological stimulation with AICAR caused a two- to threefold activation of both isoforms of AMPK (Fig. 1, *A* and *B*). The effects of AICAR stimulation on AMPK activity were not observed 10 min after the start of incubation but became prominent by 30 min. The stimulatory effect of AICAR was maximal at 40 min (Fig. 1*B*) in a dose-dependent manner (Fig. 1*A*). Therefore, we judged that stimulation with 2 mM AICAR for 40 min causes maximal AMPK activation of both α-isoforms. We also compared AICAR- and contraction-stimulated AMPK activities. Both treatments caused almost equal increases in AMPK-α_1 and -α_2 activities (Fig. 1*C*).

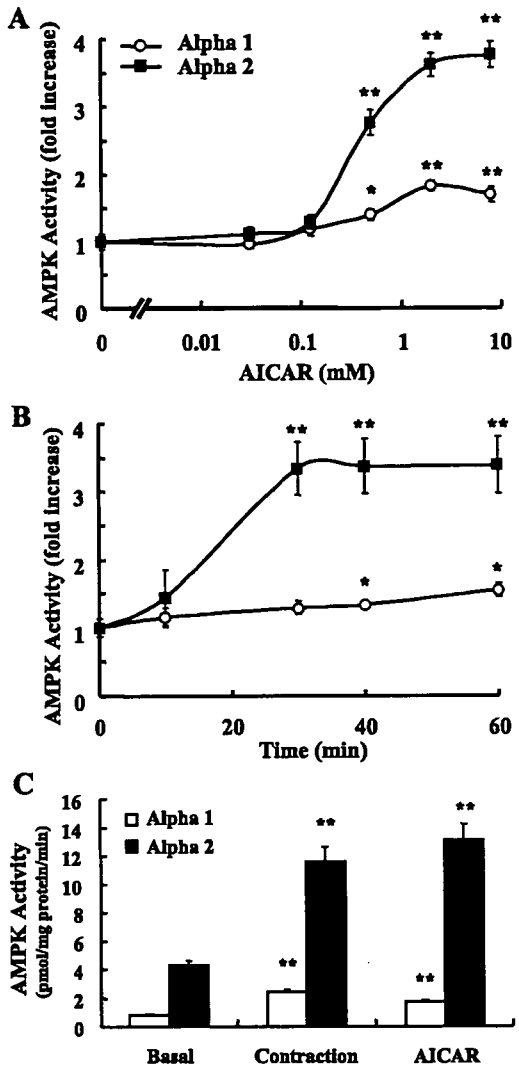

Fig. 1. Changes in α_1- and α_2-isoform-specific 5′-AMP-activated protein kinase (AMPK) activities in rat epitrochlearis muscle. Isolated muscles were incubated and stimulated by 0.03–8 mM 5-aminoimidazole-4-carboxamide-1-β-D-ribonucleoside (AICAR) for 40 min (*A*), 2 mM AICAR for 10–60 min (*B*), and in vitro contraction (10 min) or 2 mM AICAR for 40 min (*C*). Values are means ± SE (n = 4–6/group). *$P < 0.05$; **$P < 0.01$ vs. basal.

Contraction and AICAR activate glucose uptake to similar levels, comparable to the level achieved by a maximally effective dose of insulin. We determined whether muscle contraction and AICAR stimulation, both of which activate AMPK to similar levels (Fig. 1), increase glucose uptake. The almost identical four- to fivefold increases in 3-MG uptake stimulated by muscle contraction and AICAR (Fig. 2) are similar to that achieved by stimulation with a maximally effective dose (1 μM) of insulin.

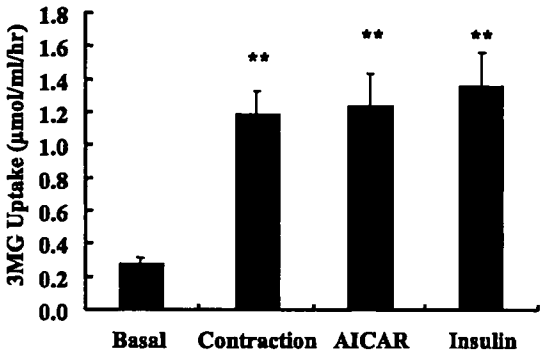

Fig. 2. 3-*O*-methylglucose (3-MG) uptake activity in rat epitrochlearis muscle. Isolated muscles were incubated and stimulated by in vitro contraction (10 min), 2 mM AICAR for 40 min, or 1 μM insulin for 40 min. Values are means ± SE (n = 5–10/group). $^{**}P < 0.01$ vs. basal.

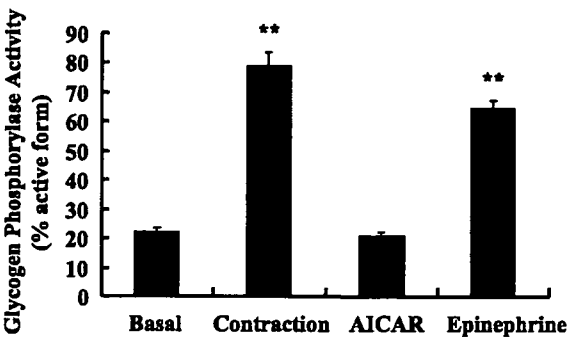

Fig. 4. Glycogen phosphorylase (GP) activity in rat epitrochlearis muscle. Isolated muscles were incubated and stimulated by in vitro contraction (10 min), 2 mM AICAR for 40 min, or 3 μg/ml epinephrine for 15 min. Values are means ± SE (n = 6–14/group). $^{**}P < 0.01$ vs. basal.

Contraction activates, but AICAR inhibits GS activity. To determine whether the activation of AMPK affects the activity of GS, the rate-limiting enzyme of glycogen synthesis, we measured GS activity. Whereas muscle contraction caused a marked increase in GS activity, AICAR stimulation conversely decreased GS activity (Fig. 3*A*). Insulin also increased GS activity, but the effect of insulin was antagonized by the presence of AICAR [active form ratio (%) = 28.0 ± 1.0 (basal), 52.7 ± 1.5 (contraction), 24.4 ± 1.1 (AICAR), 36.1 ± 2.0 (AICAR + insulin), and 45.4 ± 1.5 (insulin); Fig. 3*A*]. AICAR-induced GS inactivation was dose dependent (Fig. 3*B*), in parallel with AMPK activity (Fig. 1*A*).

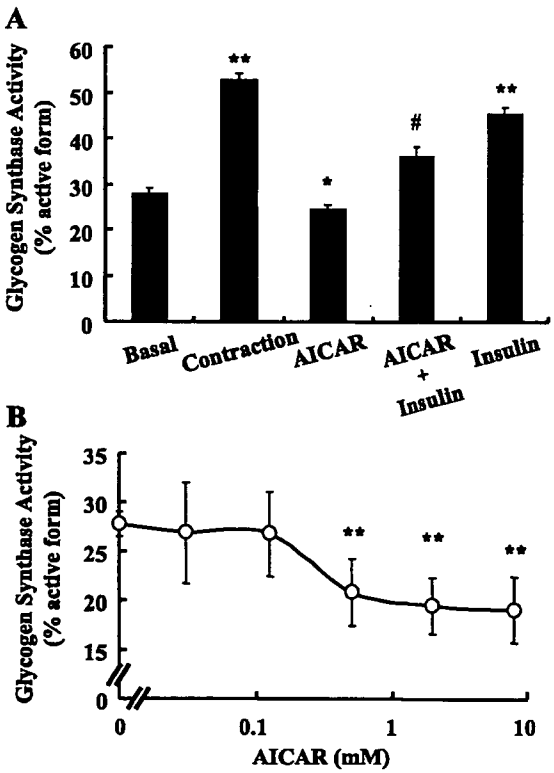

Fig. 3. Glycogen synthase (GS) activity in rat epitrochlearis muscle. *A*: isolated muscles were stimulated by in vitro contraction (10 min), 2 mM AICAR for 40 min, 2 mM AICAR + 1 μM insulin for 40 min, or 1 μM insulin. Values are means ± SE (n = 12–19/group). $^{*}P < 0.05$; $^{**}P < 0.01$ vs. basal. $^{\#}P < 0.01$ vs. insulin. *B*: muscles were incubated and stimulated by 0.03–8 mM AICAR for 40 min. Values are means ± SE [n = 4–6/group, except basal (n = 19)]. $^{**}P < 0.01$ vs. basal.

Contraction activates, but AICAR does not alter, GP activity. To determine the effect of AMPK activation on glycogenolysis, we examined the effect of AICAR stimulation on the activity of GP, which is the rate-limiting enzyme of glycogenolysis. Whereas muscle contraction and epinephrine stimulation markedly increased GP activity, AICAR did not alter GP activity [active form ratio (%) = 22.4 ± 1.0 (basal), 78.8 ± 4.4 (contraction), 20.5 ± 1.4 (AICAR), and 64.5 ± 1.7 (epinephrine); Fig. 4].

Contraction decreases, but AICAR does not alter, muscle glycogen content. We examined the effect of AICAR-stimulated AMPK activation on the concentration of glycogen. Glycogen content was reduced in contracting and epinephrine-stimulated muscles. In contrast, glycogen was unchanged by AICAR (23.3 ± 1.3, 12.4 ± 0.9, 25.6 ± 1.3, 23.7 ± 1.2, and 13.1 ± 2.4 μmol glucosyl unit/g wet muscle wt for the basal state, contraction, AICAR, insulin, and epinephrine, respectively; Fig. 5). These results are consistent with the increase in GP activity induced by contraction or epinephrine, which was unchanged by AICAR (Fig. 4).

AICAR increases lactate release from muscle. Because AICAR stimulation resulted in the inactivation of GS, despite a marked increase in glucose uptake, we investigated the amount of lactate released into the incubation buffer to clarify

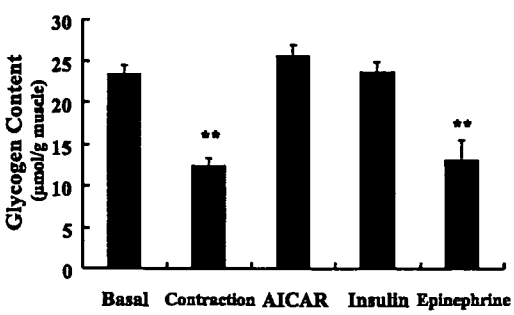

Fig. 5. Glycogen content in rat epitrochlearis muscle. Isolated muscles were incubated and stimulated by in vitro contraction (10 min), 2 mM AICAR for 40 min, 1 μM insulin for 40 min, or 3 μg/ml epinephrine for 15 min. Values are means ± SE [n = 16–20/group, except epinephrine (n = 4)]. $^{**}P < 0.01$ vs. basal.